

AD-A124 695

THEORETICAL DETERMINATION OF THE LIFT OF A SIMULATED
EJECTOR WING(U) AIR FORCE INST OF TECH WRIGHT-PATTERSON
AFB OH SCHOOL OF ENGINEERING J T DOMALSKI DEC 82

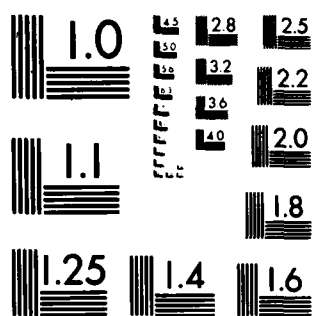
1/1

UNCLASSIFIED AFIT/GAE-82D-10

F/G 12/1

NL

END
DATE
FILMED
F B I
DTIC



MICROCOPY RESOLUTION TEST CHART
NATIONAL BUREAU OF STANDARDS-1963-A

ADA 124695

(1)

THEORETICAL DETERMINATION OF THE
LIFT OF A SIMULATED
EJECTOR WING

THESIS

AFIT/GAE-82D-10

JOHN T. DOMALSKI

DTIC
ELECTE
S FEB 22 1983 D
A

Approved for public release; distribution unlimited.

AFIT/GAE/82-D-10

THEORETICAL DETERMINATION OF THE
LIFT OF A SIMULATED
EJECTOR WING

THESIS

Presented to the Faculty of the School of Engineering
of the Air Force Institute of Technology
Air University
in Partial Fulfillment of the
Requirements for the Degree of
Master of Science

by
JOHN T. DOMALSKI
December 1982

Accession For
NTIS GRA&I
UNCLASSIFIED
CONFIDENTIAL
DISC
COPY
INSTRUCTIONS
A

Approved for public release; distribution unlimited.

Preface

The ability to predict the aerodynamic characteristics of a flight vehicle without actually fabricating and testing the vehicle has always been a highly sought-after engineering goal. Original predictions generally involved numerous, simplifying assumptions and were done via hand calculations. Today, however, the computer has greatly expanded the horizons of the theoretical aerodynamicist and has enabled him to solve much more complex and realistic problems. The work discussed herein combines the basic, time-honored principles of theoretical aerodynamics with the modern capabilities of a high-speed computing machine in order to investigate a topic of very current interest. This topic is the ejector wing; and the goal has been to develop a methodology that can be used to calculate the two-dimensional lift per unit span of any ejector wing configuration. In support of this goal, a FORTRAN computer program has been created which provides the basic mechanism for making these calculations.

It is appropriate at the close of this endeavor to express appreciation to all the people who aided me throughout its duration. Primary are the members of my committee, Dr. Harold Wright, Lieutenant Colonel Michael Smith, and Lieutenant Sal Leone, whose collective encouragement and suggestions helped me over several potential stumbling points. Especially, though, I need to thank my girls, Jan, Emily, and Elizabeth, for their patience and understanding throughout this project. I assure them the time spent away from them during the past year will be made up many times over during the upcoming ones.

Contents

	<u>Page</u>
Preface.	ii
List of Figures.	iv
List of Tables	vi
List of Symbols.	vii
Abstract	ix
I. Introduction.	1
Background	1
Purpose.	5
Geometric Model,	5
II. Theory.	9
General Equation Development	9
Evaluation of Integrals.	19
III. Numerical Examples.	24
IV. Conclusions	47
V. Recommendations	48
Bibliography	49
Appendix A Computer Program Listing	50
Vita	62

List of Figures

<u>Figure</u>	<u>Page</u>
1. Leading Edge and Underside of an Ejector Wing	2
2. Three-Dimensional Ejector Wing Design	3
3. Schematic Representations of Both Conventional and Ejector Wing Cross Sections.	4
4. Schematic of Ejector Wing Model	7
5. Geometric Model of a Simulated Ejector Wing	8
6. Geometry Associated with Determining $V_{y_2}/\delta_1(\xi_1)/\eta$	13
7. Geometry Associated with Determining $V_{y_1}/\delta_2(\xi_2)/\eta$	13
8. Upper Vorticity Distribution for Control Points: 0.2, 0.5, 0.8, 1.1, 1.4.	30
9. Lower Vorticity Distribution for Control Points: 0.2, 0.5, 0.8, 1.1, 1.4.	31
10. Y-Components of Velocity over Upper Sheet for Control Points: 0.2, 0.5, 0.8, 1.1, 1.4	32
11. Y-Components of Velocity over Lower Sheet for Control Points: 0.2, 0.5, 0.8, 1.1, 1.4	33
12. Upper Vorticity Distribution for Control Points: .10, .45, .80, 1.15, 1.50.	35
13. Lower Vorticity Distribution for Control Points: .10, .45, .80, 1.15, 1.50.	36
14. Y-Components of Velocity over Upper Sheet for Control Points: .10, .45, .80, 1.15, 1.50	37
15. Y-Components of Velocity over Lower Sheet for Control Points: .10, .45, .80, 1.15, 1.50	38
16. Upper Vorticity Distribution for Control Points: .05, .40, .75, 1.10, 1.45.	39
17. Lower Vorticity Distribution for Control Points: .05, .40, .75, 1.10, 1.45.	40
18. Y-Components of Velocity over Upper Sheet for Control Points: 0.5, .40, .75, 1.10, 1.45	41

FigurePage

19. Y-Components of Velocity over Lower Sheet for Control Points:
.05, .40, .75, 1.10, 1.45 42
20. Upper Vorticity Distribution for Control Points: .10, .30, .50,
.70, .90. 43
21. Lower Vorticity Distribution for Control Points: .10, .30, .50
.70, .90. 44
22. Y-Components of Velocity over Upper Sheet for Control Points:
.10, .30, .50, .70, .90 45
23. Y-Components of Velocity over Lower Sheet for Control Points:
.10, .30, .50, .70, .90 46

List of Tables

<u>Table</u>		<u>Page</u>
I.	Expansion of Integrals of the Form, $\int \frac{\xi^n d\xi}{a+b\xi}$, for $0 \leq n \leq 9$	22
II.	Lift Calculations Resulting from Four Different Control Point Selections for Fifth Order Truncations.	34

List of Symbols

A_n	coefficients of upper vorticity function.
B_n	coefficients of lower vorticity function.
$[AB]$	vector containing values of A_n and B_n .
\dot{A}	two-dimensional area rate of flow (ft^2/sec).
c	chord length of upper airfoil.
f_n	value of a function at any point within its domain.
l	chord length of lower airfoil.
L'	lift per unit span.
$N_{\text{lower}}, N_{\text{upper}}$	constants containing the velocity contributions due to the sink and source.
$[N]$	vector containing values of N_{lower} and N_{upper} .
n	any non-negative integer.
r	radius vector.
$[U]$	matrix containing values of integrals.
$U_{i,j}$	elements of U matrix.
$\gamma_1(\xi_1)$	upper vorticity distribution.
$\gamma_2(\xi_2)$	lower vorticity distribution.
$d\xi_1$	incremental element of vorticity on the upper sheet.
$d\xi_2$	incremental element of vorticity on the lower sheet.
ξ_1	horizontal distance along upper sheet.
ξ_2	horizontal distance along lower sheet.
$dV_{y_1/d\xi_1}$	incremental velocity induced at a point on the upper sheet by $d\xi_1$.
$V_{y_1/r_1(\xi_1)}$	velocity induced at a point on the upper sheet by $\gamma_1(\xi_1)$.
$dV_{y_2/d\xi_2}$	incremental velocity induced at a point on the lower sheet by $d\xi_2$.

$V_{y_2/\zeta_2(\zeta_2)}$	velocity induced at a point on the lower sheet by $\gamma_2(\zeta_2)$.
$dV_{y_2/d\zeta_1}$	incremental velocity induced at a point on the lower sheet by $d\zeta_1$.
$dV_{y_2/d\zeta_1/n}$	normal component of $dV_{y_2/d\zeta_1}$.
$V_{y_2/\zeta_1(\zeta_1)/n}$	normal component of velocity at a point on the lower sheet induced by $\gamma_1(\zeta_1)$.
$dV_{y_1/d\zeta_2}$	incremental velocity induced at a point on the upper sheet by $d\zeta_2$.
$dV_{y_1/d\zeta_2/n}$	normal component of $dV_{y_1/d\zeta_2}$.
$V_{y_1/\zeta_2(\zeta_2)/n}$	normal component of velocity at a point on the upper sheet induced by $\gamma_2(\zeta_2)$.
V_∞	free stream velocity.
v	y-component of velocity
x_1	horizontal location of sink.
x_2	horizontal location of source.
x_3	horizontal location of leading edge of lower chord line.
x_4	horizontal location of trailing edge of lower chord line.
y_1	vertical location of upper chord line.
y_2	vertical location of lower chord line.
β	angle associated with $V_{y_2/\zeta_1(\zeta_1)/n}$
δ	angle associated with $V_{y_1/\zeta_2(\zeta_2)/n}$
Δ	$\frac{\cos [\tan^{-1} (\frac{y_1 - y_2}{x - x_3 - \zeta_2})]}{\sqrt{(x - x_3 - \zeta_2)^2 + (y_1 - y_2)^2}}$
Θ	$\frac{\cos [\tan^{-1} (\frac{y_1 - y_2}{x - \zeta_1})]}{\sqrt{(x - \zeta_1)^2 + (y_1 - y_2)^2}}$
ϕ	velocity potential.
Λ_{sink}	strength of the sink.
Λ_{source}	strength of the source.
ρ	density.

Abstract

The theoretical framework and general solution procedure have been developed for calculation of the lift per unit span of an ejector wing model. This model is based on the fundamentals of Potential Flow and Thin Airfoil Theory and incorporates a point sink, point source, and two bound vortex sheets. The solution procedure consistently satisfies both the flow tangency and Kutta conditions, but its usefulness is shown to be highly dependent on the number of control points used. Numerical examples are presented for cases involving five control points, and the lift calculations which result are shown to be inconsistent. A FORTRAN computer program is included for the five control point case, but it can be modified to accommodate any number of control points.

THEORETICAL DETERMINATION OF THE LIFT OF A SIMULATED EJECTOR WING

I. Introduction

Background

An ejector wing looks much like a conventional subsonic aircraft wing except for the presence of one or more slots which run along its span-wise direction. Figure 1 shows an actual ejector wing that has recently been tested in the 7' x 10' Army tunnel at the NASA Ames Research Center (7). The figure shows the underside and leading edge of the wing and the presence of four distinct slots. These slots occupy what would be the interior region of a conventional wing, and they exit at the top surface near the trailing edge. Figure 2 is a cut-away drawing of the wing showing both its external and internal configurations (7). Figure 3 shows schematic representations of the cross sections of both conventional and ejector wings.

The principle upon which the design of an ejector wing is based involves the injection of high energy air into the slots. This air is obtained from the aircraft's exhaust, and it is mixed with the air flowing through the slots. When this mixture reaches the wing's upper surface, it acts to delay the onset of boundary layer separation. By keeping the flow attached to the ejector wing's surface over a greater area, an increase in lift over that of a conventional wing is obtained.

The particular wing design shown in Figures 1 and 2 was first proposed by the Flight Dynamics Laboratory of the Air Force Wright Aeronautical Laboratories at Wright-Patterson Air Force Base, Ohio. It was designed

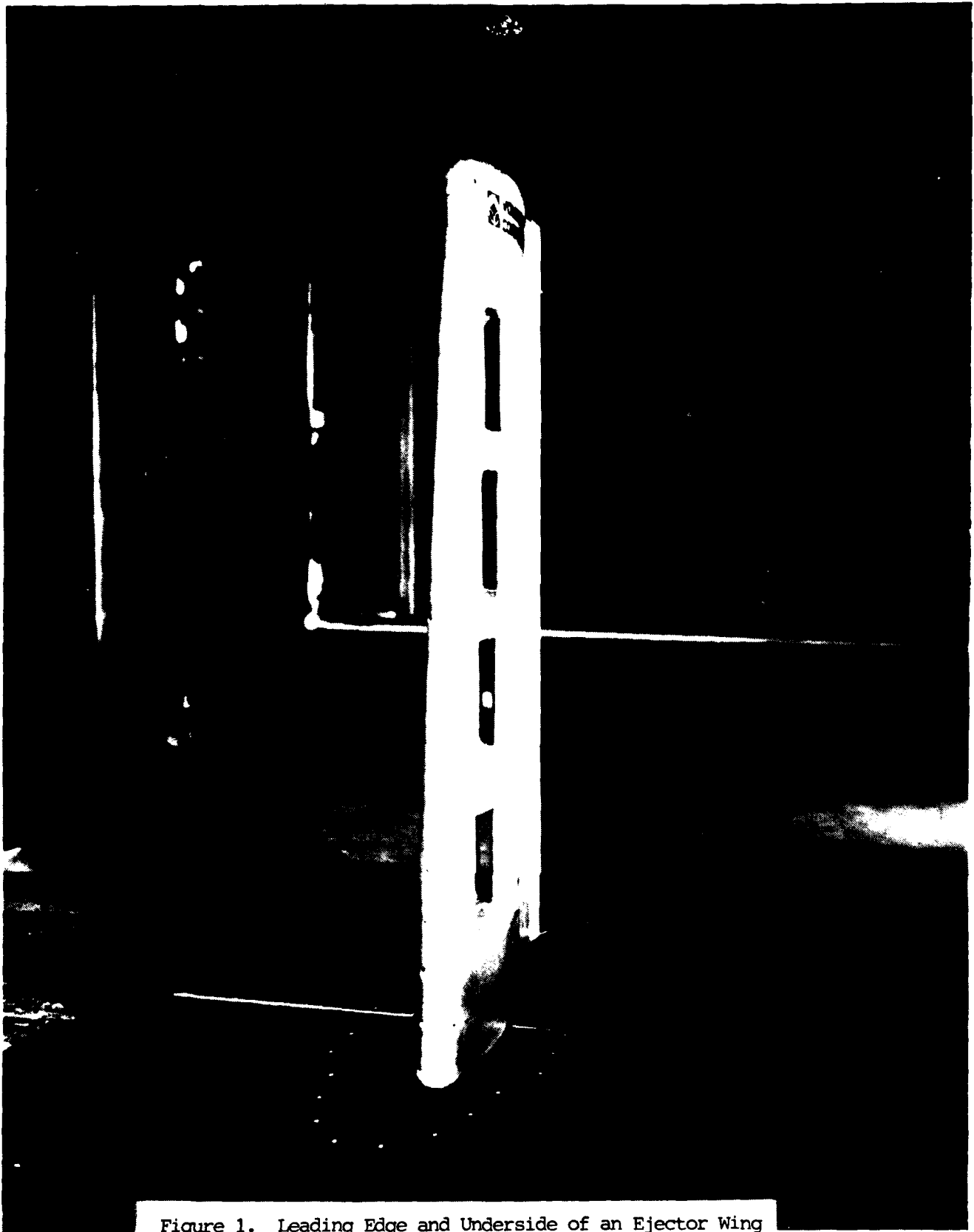


Figure 1. Leading Edge and Underside of an Ejector Wing

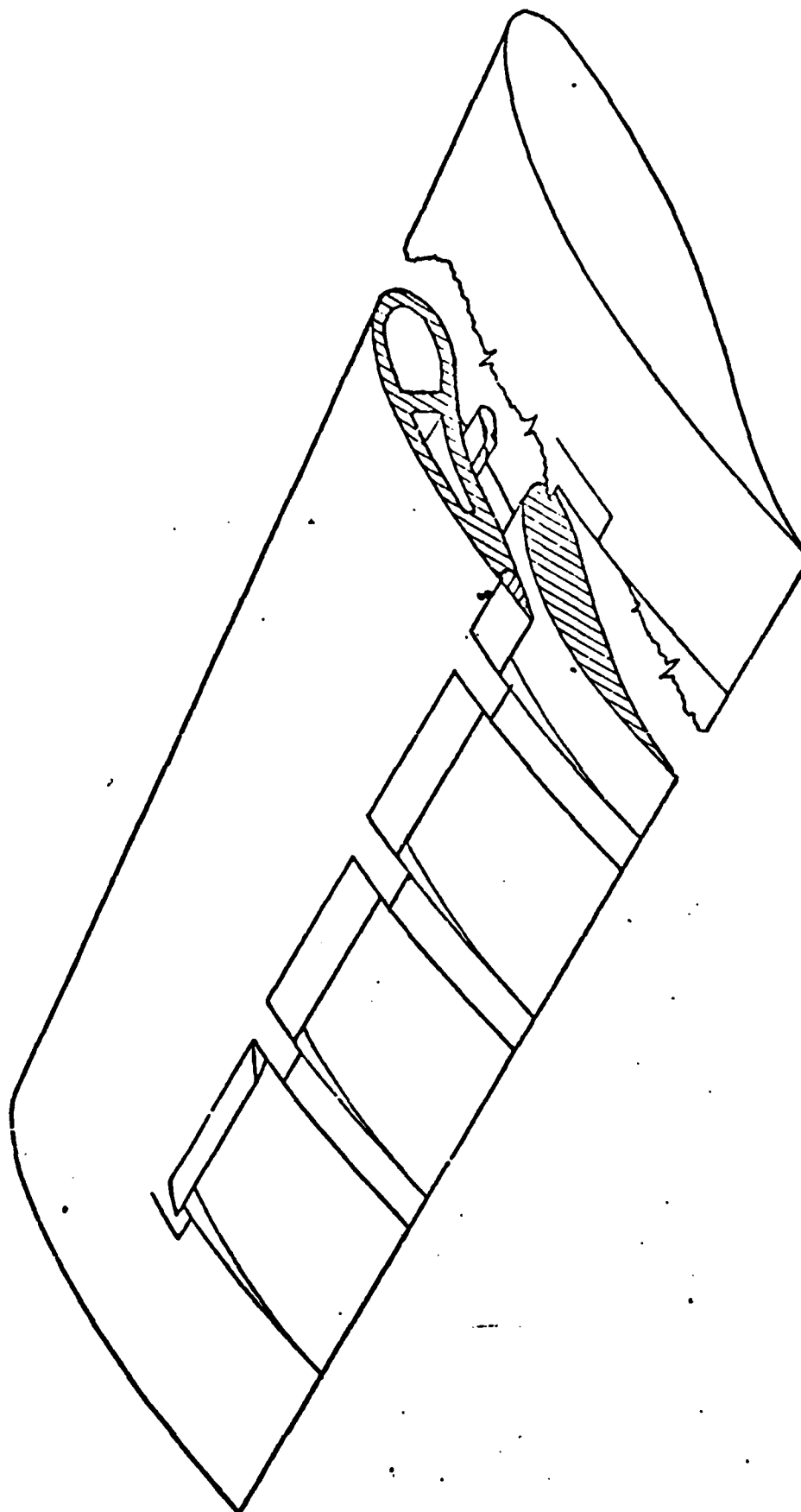


Figure 2. Three-Dimensional Ejector Wing Design

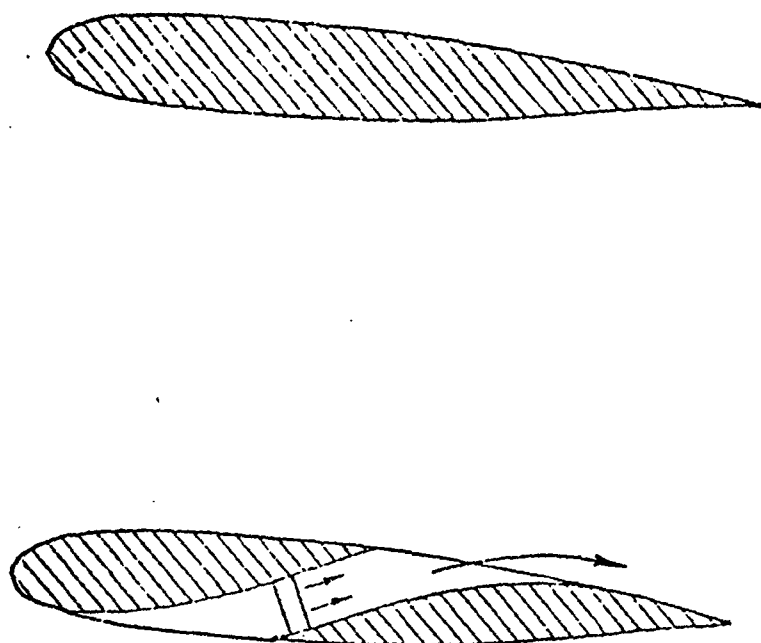


Figure 3. Schematic Representations of Both Conventional and Ejector Wing Cross Sections

using methodologies incorporating three-dimensional vortex-lattice and lifting line theories and two-dimensional analog techniques which were coupled with boundary layer prediction methods and empirically-based ejector augmentor design and performance procedures. The objective of the design was to produce a wing which would achieve high lift over a range of high angles of attack in subsonic flight up to Mach numbers of 0.3 (7).

Purpose

As an aide to assessing the data generated by the testing of this wing, it was requested that a simple theoretical model of an ejector wing be developed. This model, hopefully, would enable quick and easy determination of the effects on the lift of the wing that result from varying its geometric characteristics. These characteristics include, for example:

- the height of the slot (i.e., the vertical distance between the upper and lower airfoil sections)
- the horizontal distance between the leading edges of the two airfoils
- the length of the lower airfoil with respect to the upper

The development of this model is the objective of this thesis. The methodology of the development and the results obtained are discussed below.

Geometric Model

A two-dimensional geometric model was constructed as shown in Figure 4. It was based upon a two-element lifting surface; with a sink and source to represent the ejector inlet and exhaust mass flows, respectively (5, 6, 9). It was decided to simulate the upper and lower airfoil sections as parallel symmetric airfoils and to represent them by their chord lines. Each chord line was assumed to be of unit length, and the leading edge of the lower line was selected to be 0.55 unit behind the leading edge of the upper line.

(Orientation of the two surface elements was arbitrary (8).) This resulted in an overall chord length for the simulated ejector wing of 1.55 units. The vertical spacing between the lines was assumed to be about one-tenth of their collective horizontal length (7). Thus, a vertical spacing of 0.15 unit was selected.

The horizontal location of the sink was determined by placing it near the leading edge of the lower line; at a distance of 0.05 unit in front of the lower line. The horizontal location of the source was determined by placing it midway between the trailing edges of the lines. The vertical locations of both were established by placing them midway between the chord lines.

Figure 5 shows the complete geometric model of the ejector wing and identifies all the numerical constants that are involved in defining its configuration. The configuration is drawn with respect to a universal X-Y coordinate system, but it should be noted at this time that two other coordinate systems also are present. They have significance only in the horizontal direction and they have origins at the leading edges of the chord lines. They are designated the ξ_1-Y' and ξ_2-Y'' systems and will be used later to develop the mathematical model of the wing.

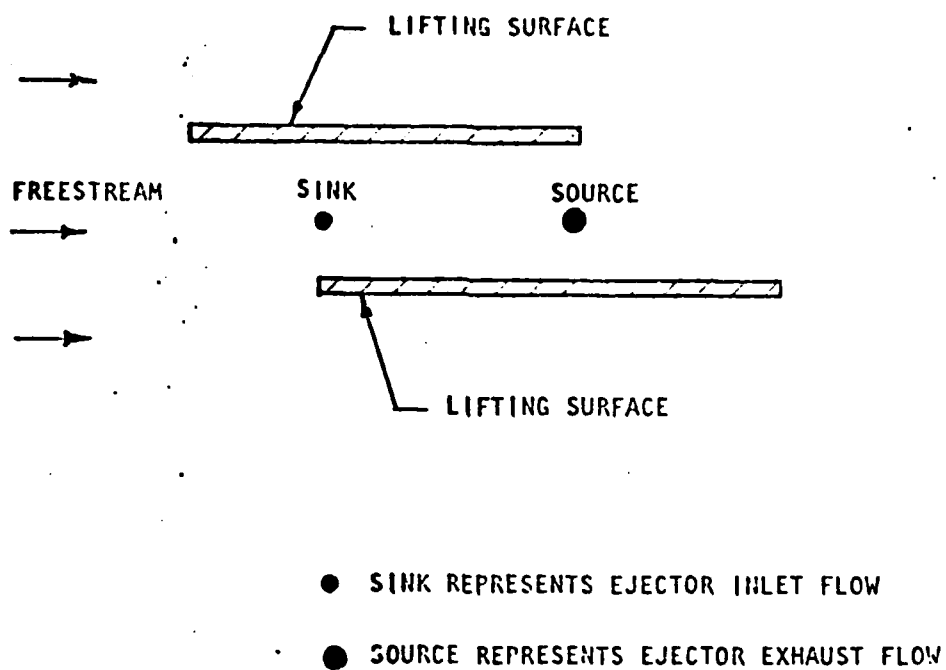
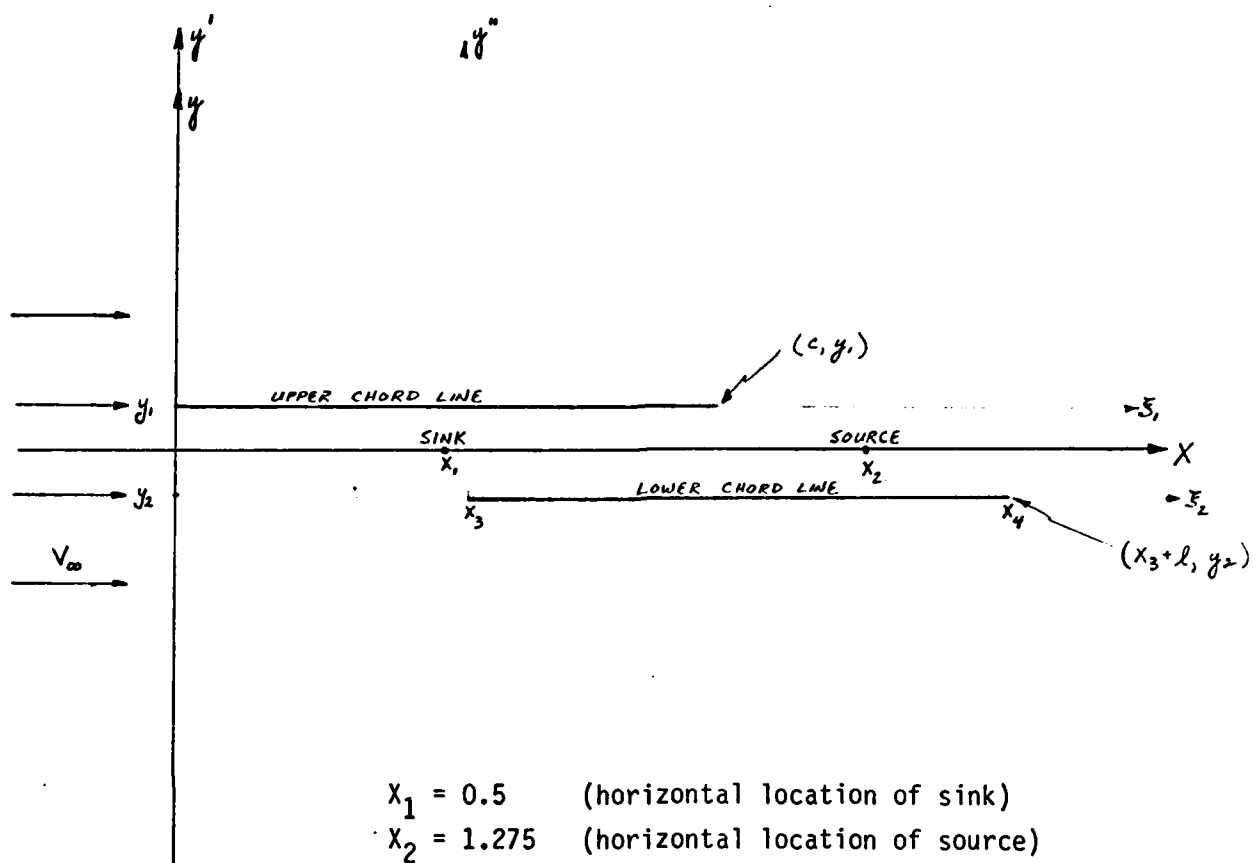


Figure 4. Schematic of Ejector Wing Model



$x_1 = 0.5$	(horizontal location of sink)
$x_2 = 1.275$	(horizontal location of source)
$x_3 = 0.55$	(horizontal location of lower leading edge)
$x_4 = 1.55$	(horizontal location of lower trailing edge)
$y_1 = 0.075$	(vertical location of upper line)
$y_2 = -0.075$	(vertical location of lower line)
$c = 1.0$	(length of upper line)
$l = 1.0$	(length of lower line)

Figure 5. Geometric Model of a Simulated Ejector Wing

II. Theory

General Equation Development

The mathematical model for an ejector wing was developed from consideration of the principles of low-speed aerodynamics. Central to this development was the assumption that the viscous boundary layer surrounding the wing was thin and, therefore, had a negligible influence on the inviscid flow field (1). In addition to ignoring the effects of viscosity, it was also assumed that the flow about the wing was steady, incompressible, and irrotational. Thus, for this combination of conditions, the governing equation for the flow field is Laplace's Equation:

$$\nabla^2 \phi = 0 \quad (1)$$

where ϕ is the total velocity potential (1).

The model was constructed by the addition of a point sink, a point source, and two parallel vortex sheets to a uniform stream. The vortex sheets are needed on the chord lines in order to produce a lift-generating pressure difference between the upper and lower surfaces of the airfoils they represent. The vortex sheets are parallel to the uniform stream and the sink and source are located in the area between them. The procedure used to develop the model began with determining expressions for the y-components of velocity (v) at all points on the sheets. Since the governing equation is linear, the velocity potential at any point in the field resulting from this combination of elements is simply the sum of the velocity potentials for each one (4). Therefore, the velocity at any point consists of contributions from the individual components. Thus, for the case involving no angle of attack, two scalar equations for v result:

$$v_{\text{upper sheet}} = v_{\text{sink}} + v_{\text{source}} + v_{\text{upper vorticity distribution}} + v_{\text{lower vorticity distribution}} \quad (2)$$

$$v_{\text{lower sheet}} = v_{\text{sink}} + v_{\text{source}} + v_{\text{upper vorticity distribution}} + v_{\text{lower vorticity distribution}} \quad (3)$$

Considering first the contributions of the sink and the source, an expression for the velocity potential at any point (x, y) in the flow field is:

$$\phi = \phi_{\text{sink}} + \phi_{\text{source}} \quad (4)$$

where:

$$\phi_{\text{sink}} = - \frac{\Lambda_{\text{sink}}}{2\pi} \ln r_a \quad \text{and} \quad (5)$$

$$\phi_{\text{source}} = \frac{\Lambda_{\text{source}}}{2\pi} \ln r_b \quad (6)$$

For points on the sheets, expressions for r_a and r_b in terms of x and y can be written. They are:

$$r_a = \sqrt{(x - x_1)^2 + y^2} \quad \text{and} \quad (7)$$

$$r_b = \sqrt{(x - x_2)^2 + y^2} \quad (8)$$

Substituting into the expression for ϕ , gives:

$$\phi = - \frac{\Lambda_{\text{sink}}}{2\pi} \ln \sqrt{x^2 - 2x_1x + x_1^2 + y^2} + \frac{\Lambda_{\text{source}}}{2\pi} \ln \sqrt{x^2 - 2x_2x + x_2^2 + y^2} \quad (9)$$

An expression for v is obtained by differentiating this expression with respect to y . Thus:

$$v = \partial\phi/\partial y \quad (10)$$

$$v = - \frac{\Lambda_{\text{sink}}}{2\pi} \left[\frac{y}{x^2 - 2x_1x + x_1^2 + y^2} \right] + \frac{\Lambda_{\text{source}}}{2\pi} \left[\frac{y}{x^2 - 2x_2x + x_2^2 + y^2} \right] \quad (11)$$

Next to be considered are the velocities induced by the vortex sheets at points on the sheets, themselves. It is known that these velocities are perpendicular to the sheets (1). Considering an incremental element of the upper vorticity distribution ($d\xi_1$), the incremental velocity it induces at a point on the upper sheet; namely at (x, y_1) is:

$$dV_{y_1}/d\xi_1 = \frac{\gamma_1(\xi_1) d\xi_1}{2\pi r_1} \quad (12)$$

where:

$\gamma_1(\xi_1)$ = upper vorticity distribution

$$r_1 = x - \xi_1$$

Substituting for r_1 in Equation (12) and integrating over the entire length of the upper sheet leads to:

$$V_{y_1/\gamma_1(\xi_1)} = \frac{1}{2\pi} \int_0^c \frac{\gamma_1(\xi_1)}{x - \xi_1} d\xi_1 \quad (13)$$

Likewise for the lower sheet, consider the incremental velocity induced by $d\xi_2$ at a point, (x, y_2) . Integrating over the entire length of the lower sheet leads to:

$$V_{y_2/\gamma_2(\xi_2)} = \int_{x_3}^{x_4} \frac{\gamma_2(\xi_2)}{2\pi r_2} d\xi_2 = \frac{1}{2\pi} \int_0^{x_4-x_3} \frac{\gamma_2(\xi_2)}{x-x_3-\xi_2} d\xi_2 \quad (14)$$

Again, this velocity is perpendicular to the sheet and thus, is in the y -direction.

Additional complexity is found when considering the velocities induced by $d\xi_1$ at points on the lower sheet and by $d\xi_2$ at points on the upper sheet. This complexity is caused by the geometry of the model but is easily handled by separating and focusing on the components of the induced velocities that are normal to the sheets, only.

Consider the velocities induced at points on the lower sheet by $d\xi_1$ (See Figure 6). For this case, the velocity in question is:

$$dV_{y2}/d\xi_1 = \frac{\gamma_1(\xi_1) d\xi_1}{2\pi r_3} \quad (15)$$

where:

$$r_3 = \sqrt{(x - \xi_1)^2 + (y_1 - y_2)^2} \quad (16)$$

The angle, β , is involved in defining the normal component of this velocity and this angle is defined as:

$$\beta = \tan^{-1} \left(\frac{y_1 - y_2}{x - \xi_1} \right) \quad (17)$$

Thus, the normal component of velocity is:

$$dV_{y2}/d\xi_1/n = \frac{\gamma_1(\xi_1)}{2\pi r_3} d\xi_1 \cos \beta \quad (18)$$

Integrating over the length of the upper sheet gives:

$$V_{y2/\gamma_1(\xi_1)/n} = \frac{1}{2\pi} \int_0^c \frac{\gamma_1(\xi_1) \left\{ \cos \left[\tan^{-1} \left(\frac{y_1 - y_2}{x - \xi_1} \right) \right] \right\}}{\sqrt{(x - \xi_1)^2 + (y_1 - y_2)^2}} d\xi_1 \quad (19)$$

Likewise, the velocities induced at points on the upper sheet by $d\xi_2$ are (See Figure 7):

$$dV_{y1}/d\xi_2 = \frac{\gamma_2(\xi_2) d\xi_2}{2\pi r_4} \quad (20)$$

where:

$$r_4 = \sqrt{(x - x_3 - \xi_2)^2 + (y_1 - y_2)^2} \quad (21)$$

The angle δ is involved in defining the normal component and this angle is defined as:

$$\delta = \tan^{-1} \left(\frac{y_1 - y_2}{x - x_3 - \xi_2} \right)$$

The normal component of the incremental velocity then is seen to be:

$$dV_{y1}/d\xi_2/n = \frac{\gamma_2(\xi_2)}{2\pi r_4} d\xi_2 \cos \delta$$

Integrating over the length of the lower sheet gives:

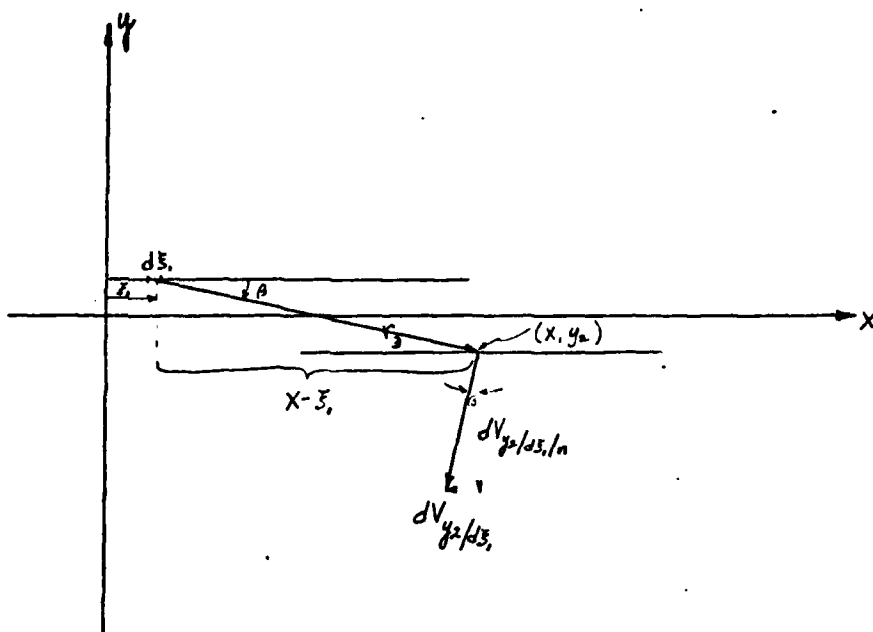


Figure 6. Geometry Associated with Determining $V_{y2}/\delta_1(\xi_1)/n$

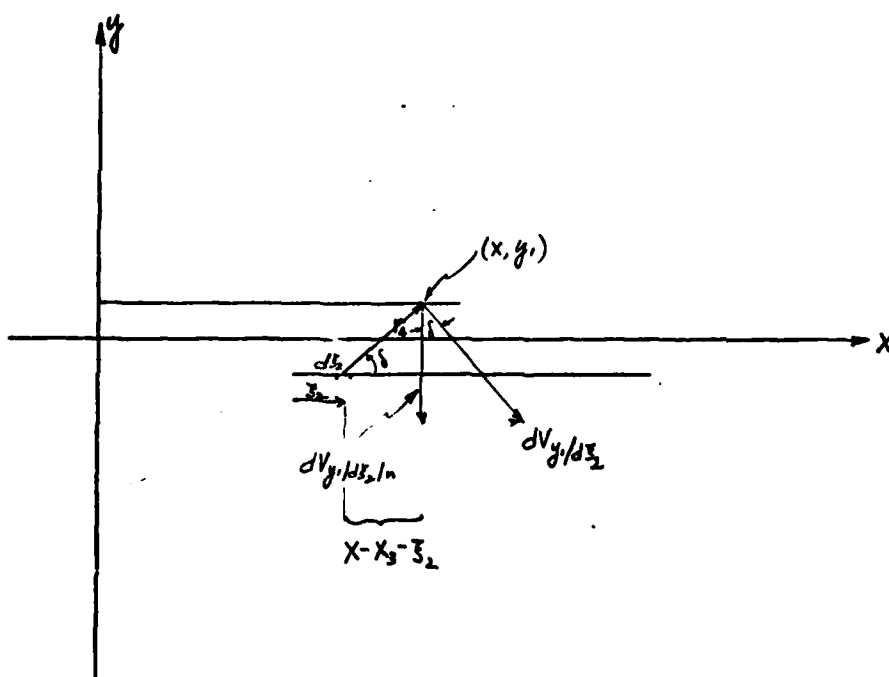


Figure 7. Geometry Associated with Determining $V_{y1}/\delta_2(\xi_2)/n$

$$V_{y, \gamma_2(\xi_2)/n} = \frac{1}{2\pi} \int_0^{x_4-x_3} \frac{\gamma_2(\xi_2) \left\{ \cos \left[\tan^{-1} \left(\frac{y_1 - y_2}{x - x_3 - \xi_2} \right) \right] \right\}}{\sqrt{(x - x_3 - \xi_2)^2 + (y_1 + y_2)^2}} d\xi_2 \quad (22)$$

In order to find the total y-components of velocity at points on the vortex sheets, it is necessary to sum the contributions from all the elements in the model as per Equations (2) and (3). Thus, for the upper sheet:

$$V_{\text{upper sheet}} = \frac{\Gamma_{\text{source}}}{2\pi} \left[\frac{y_1}{x^2 - 2x_2x + x_2^2 + y_1^2} \right] - \frac{\Gamma_{\text{sink}}}{2\pi} \left[\frac{y_1}{x^2 - 2x_1x + x_1^2 + y_1^2} \right] + \frac{1}{2\pi} \int_0^c \frac{\gamma_1(\xi_1)}{x - \xi_1} d\xi_1 + \frac{1}{2\pi} \int_0^{x_4-x_3} \frac{\gamma_2(\xi_2) \left\{ \cos \left[\tan^{-1} \left(\frac{y_1 - y_2}{x - x_3 - \xi_2} \right) \right] \right\}}{\sqrt{(x - x_3 - \xi_2)^2 + (y_1 - y_2)^2}} d\xi_2 \quad (23)$$

And for the lower sheet:

$$V_{\text{lower sheet}} = \frac{\Gamma_{\text{source}}}{2\pi} \left[\frac{y_2}{x^2 - 2x_2x + x_2^2 + y_2^2} \right] - \frac{\Gamma_{\text{sink}}}{2\pi} \left[\frac{y_2}{x^2 - 2x_1x + x_1^2 + y_2^2} \right] + \frac{1}{2\pi} \int_0^c \frac{\gamma_1(\xi_1) \left\{ \cos \left[\tan^{-1} \left(\frac{y_1 - y_2}{x - \xi_1} \right) \right] \right\}}{\sqrt{(x - \xi_1)^2 + (y_1 - y_2)^2}} d\xi_1 + \frac{1}{2\pi} \int_0^{x_4-x_3} \frac{\gamma_2(\xi_2)}{x - x_3 - \xi_2} d\xi_2 \quad (24)$$

Equations 23 and 24 are the heart of the ejector wing model, and the method of their solution is the key to determining the lift per unit span of such a wing. The method of solution used involved satisfying both a boundary condition and an auxiliary condition and assuming algebraic forms for the two unknown vorticity distributions: $\gamma_1(\xi_1)$ and $\gamma_2(\xi_2)$.

First, the boundary condition. In order to make the geometric model actually representative of the aerodynamic characteristics of an ejector wing, Thin-Airfoil Theory states that the camber lines (which for the case of symmetric airfoils are coincident with the chord lines) must be streamlines of the flow field. In order to make the camber/chord lines

streamlines, it is necessary that all velocity components normal to them be zero (1). This is the flow-tangency condition and its imposition on Equations (23) and (24) gives:

$$\begin{aligned} & \perp_{\text{source}} \left[\frac{y_1}{x^2 - 2x_2x + x_2^2 + y_1^2} \right] - \perp_{\text{sink}} \left[\frac{y_1}{x^2 - 2x_1x + x_1^2 + y_1^2} \right] + \\ & \int_0^c \frac{\gamma_1(\xi_1)}{x - \xi_1} d\xi_1 + \int_0^{x_4 - x_3} \frac{\gamma_2(\xi_2) \left\{ \cos \left[\tan^{-1} \left(\frac{y_1 - y_2}{x - x_3 - \xi_2} \right) \right] \right\}}{\sqrt{(x - x_3 - \xi_2)^2 + (y_1 - y_2)^2}} d\xi_2 = 0 \end{aligned} \quad (25)$$

$$\begin{aligned} & \perp_{\text{source}} \left[\frac{y_2}{x^2 - 2x_2x + x_2^2 + y_2^2} \right] - \perp_{\text{sink}} \left[\frac{y_2}{x^2 - 2x_1x + x_1^2 + y_2^2} \right] + \\ & \int_0^c \frac{\gamma_1(\xi_1) \left\{ \cos \left[\tan^{-1} \left(\frac{y_1 - y_2}{x - \xi_1} \right) \right] \right\}}{\sqrt{(x - \xi_1)^2 + (y_1 - y_2)^2}} d\xi_1 + \int_0^{x_4 - x_3} \frac{\gamma_2(\xi_2)}{x - x_3 - \xi_2} d\xi_2 = 0 \end{aligned} \quad (26)$$

The auxiliary boundary condition is the Kutta condition which demands that the vorticity distributions at the trailing edges of the airfoils be zero (1). This condition was satisfied through specification of the coefficients of the functional expressions assumed for $\gamma_1(\xi_1)$ and $\gamma_2(\xi_2)$.

It was decided to use power series representations for both of these functions and to expand the series about the trailing edges of the airfoils.

Thus, $\gamma_1(\xi_1)$ is:

$$\gamma_1(\xi_1) = A_0 + A_1(\xi_1 - c) + A_2(\xi_1 - c)^2 + \dots + A_n(\xi_1 - c)^n + \dots \quad (27)$$

where c is the length of the upper sheet. Similarly, $\gamma_2(\xi_2)$ is:

$$\gamma_2(\xi_2) = B_0 + B_1(\xi_2 - l) + B_2(\xi_2 - l)^2 + \dots + B_n(\xi_2 - l)^n + \dots \quad (28)$$

where l is the length of the lower sheet.

By assuming that $\gamma_1(\xi_1)$ and $\gamma_2(\xi_2)$ both are able to be represented by power series, it has further been assumed that all points on the sheets lie within the convergence sets of two series. The result of these assumptions is that both $\gamma_1(\xi_1)$ and $\gamma_2(\xi_2)$ are continuous over the lengths of the sheets. As will be shown later, these two functions are indeed continuous over the lengths of the sheets thereby justifying the assumptions made.

The Kutta condition demands that $\gamma_1(c) = 0$ and $\gamma_2(\ell) = 0$. These conditions are satisfied by setting both A_0 and B_0 equal to zero. Thus, the series reduce to:

$$\gamma_1(\xi_1) = A_1(\xi_1 - c) + A_2(\xi_1 - c)^2 + \dots + A_n(\xi_1 - c)^n + \dots \quad (29)$$

and

$$\gamma_2(\xi_2) = B_1(\xi_2 - \ell) + B_2(\xi_2 - \ell)^2 + \dots + B_n(\xi_2 - \ell)^n + \dots \quad (30)$$

The next step in the solution of the two major equations of the model, Equations (25) and (26), involves substitution of Equations (29) and (30) into them and the subsequent determination of A_1 through A_n and B_1 through B_n which force the vortex sheets to become streamlines of the flow field. These coefficients are, of course, infinite in number and, therefore, require an infinite number of equations for their complete determination. Needless to say, this is an impossibility and truncation of the series representations at some finite power must be done. It will be shown later that the accuracy and validity of the lift estimations calculated for the model are highly dependent on the order of the truncations used and that very high order truncations are required for believable results. However, for the present discussion, it will be assumed that no truncation is used and that an infinite number of coefficients will be determined.

From inspection of Equations (25) and (26), it is seen that the terms associated with the source and the sink take on finite values for any value of X selected. (It should be remembered that x_1 , x_2 , y_1 , y_2 , L_{source} , and L_{sink}

are all constants of the model and are assigned finite values.) Thus, in order to determine values for A_1 through A_n and B_1 through B_n , it is necessary to evaluate the sink- and source-induced velocities at n different values of X . This is easily done and the values which result are labeled N_{upper} and N_{lower} . Equations (25) and (26) then become:

$$\int_0^c \frac{\gamma_1(\xi_1)}{X - \xi_1} d\xi_1 + \int_0^l \frac{\gamma_2(\xi_2) \left\{ \cos \left[\tan^{-1} \left(\frac{y_1 - y_2}{X - X_3 - \xi_2} \right) \right] \right\}}{\sqrt{(X - X_3 - \xi_2)^2 + (y_1 - y_2)^2}} d\xi_2 = N_{upper} \quad (31)$$

$$\int_0^c \frac{\gamma_1(\xi_1) \left\{ \cos \left[\tan^{-1} \left(\frac{y_1 - y_2}{X - \xi_1} \right) \right] \right\}}{\sqrt{(X - \xi_1)^2 + (y_1 - y_2)^2}} d\xi_1 + \int_0^l \frac{\gamma_2(\xi_2)}{X - X_3 - \xi_2} d\xi_2 = N_{lower} \quad (32)$$

where:

$$N_{upper} = \mathcal{L}_{sink} \left[\frac{y_1}{X^2 - 2X_1X + X_1^2 + y_1^2} \right] - \mathcal{L}_{source} \left[\frac{y_1}{X^2 - 2X_2X + X_2^2 + y_1^2} \right] \quad (33)$$

$$N_{lower} = \mathcal{L}_{sink} \left[\frac{y_2}{X^2 - 2X_1X + X_1^2 + y_2^2} \right] - \mathcal{L}_{source} \left[\frac{y_2}{X^2 - 2X_2X + X_2^2 + y_2^2} \right] \quad (34)$$

Since both N_{upper} and N_{lower} can take on an infinite number of values (i.e., one value for each value of X selected), it is the generation of these constants that enables an infinite set of algebraic equations to be formed.

Substitution of Equations (29) and (30) into Equation (31) gives:

$$\int_0^c \frac{A_1(\xi_1 - c) + A_2(\xi_1 - c)^2 + \dots + A_n(\xi_1 - c)^n}{X - \xi_1} d\xi_1 + \int_0^l \frac{[B_1(\xi_2 - l) + B_2(\xi_2 - l)^2 + \dots + B_n(\xi_2 - l)^n] \left\{ \cos \left[\tan^{-1} \left(\frac{y_1 - y_2}{X - X_3 - \xi_2} \right) \right] \right\}}{\sqrt{(X - X_3 - \xi_2)^2 + (y_1 - y_2)^2}} d\xi_2 = N_{upper} \quad (35)$$

By expanding and simplifying the integral expressions in this equation, the parent equation for a set of n algebraic equations is arrived at. Namely, this procedure leads to:

$$\begin{aligned}
& A_1 \int_0^c \frac{\xi_1 - c}{x - \xi_1} d\xi_1 + A_2 \int_0^c \frac{(\xi_1 - c)^2}{x - \xi_1} d\xi_1 + \dots + A_n \int_0^c \frac{(\xi_1 - c)^n}{x - \xi_1} d\xi_1 + \\
& B_1 \int_0^l (\xi_2 - l) \Delta d\xi_2 + B_2 \int_0^l (\xi_2 - l)^2 \Delta d\xi_2 + \dots + B_n \int_0^l (\xi_2 - l)^n \Delta d\xi_2 = N_{upper} \quad (36)
\end{aligned}$$

where $\Delta = \frac{\cos \left[\tan^{-1} \left(\frac{y_1 - y_2}{x - x_3 - \xi_2} \right) \right]}{\sqrt{(x - x_3 - \xi_2)^2 + (y_1 - y_2)^2}}$

Similar substitution, expansion, and simplification of equation (32) produces:

$$\begin{aligned}
& A_1 \int_0^c (\xi_1 - c) \Theta d\xi_1 + A_2 \int_0^c (\xi_1 - c)^2 \Theta d\xi_1 + \dots + A_n \int_0^c (\xi_1 - c)^n \Theta d\xi_1 + \\
& B_1 \int_0^l \frac{\xi_2 - l}{x - x_3 - \xi_2} d\xi_2 + B_2 \int_0^l \frac{(\xi_2 - l)^2}{x - x_3 - \xi_2} d\xi_2 + \dots + B_n \int_0^l \frac{(\xi_2 - l)^n}{x - x_3 - \xi_2} d\xi_2 = N_{lower} \quad (37)
\end{aligned}$$

where $\Theta = \frac{\cos \left[\tan^{-1} \left(\frac{y_1 - y_2}{x - \xi_1} \right) \right]}{\sqrt{(x - \xi_1)^2 + (y_1 - y_2)^2}}$

Equations (36) and (37) are much more easily represented by use of matrix notation. By designating the integrals contained in these two equations as $U_{i,j}$ and by adding the subscript, i , to the N_{upper} and N_{lower} constants, the following matrix equation is arrived at:

$$\begin{bmatrix} U_{1,1} & U_{1,2} & \dots & U_{1,n} \\ U_{2,1} & U_{2,2} & \dots & U_{2,n} \\ \vdots & \vdots & \ddots & \vdots \\ U_{n,1} & U_{n,2} & \dots & U_{n,n} \end{bmatrix} \begin{bmatrix} A_1 \\ A_2 \\ \vdots \\ A_n \\ B_1 \\ B_2 \\ \vdots \\ B_n \end{bmatrix} = \begin{bmatrix} N_{upper1} \\ N_{upper2} \\ \vdots \\ N_{uppern} \\ N_{lower1} \\ N_{lower2} \\ \vdots \\ N_{lowern} \end{bmatrix} \quad (38)$$

Or, in more compact notation:

$$[U] [AB] = [N] \quad (39)$$

The solution of this matrix equation, namely, the determination of the vector, AB, is accomplished by premultiplying the N vector by the inverted U matrix. Therefore, the solution is:

$$[AB] = [U]^{-1} [N] \quad (40)$$

As stated earlier, the coefficients, A_1 through A_n and B_1 through B_n , which comprise the AB vector, are the assumed coefficients of the two unknown vorticity functions. The values of these coefficients which result from this method of solution are the ones which cause the two vortex sheets to be streamlines of the flow field. When these coefficients are substituted into the vorticity functions, polynomials of degree, n , result. The lift per unit span of the airfoil section is then calculated from these vorticity functions according to [4]:

$$L' = \rho V_{\infty} \left[\int_0^c \gamma_1(\xi_1) d\xi_1 + \int_0^l \gamma_2(\xi_2) d\xi_2 \right] \quad (41)$$

Evaluation of Integrals

The preceding section has provided the general theory needed to establish the solution framework for the ejector wing, two-dimensional, lift calculation problem. The solution of Equation (39) was shown to be a fairly easy and straight-forward procedure. However, the problem is complicated by the need to evaluate all of the integrals shown in Equations (36) and (37) and which comprise the U matrix in Equation (39). Basically, these integrals are of two different types and are handled in two different ways. The first type is associated with the A_1 through A_n coefficients in Equation (36) and the B_1 through B_n coefficients in Equation (37). It

is of the general form:

$$\int_1^2 \frac{f(\xi)}{a - \xi} d\xi$$

and possesses a singularity at the point, $\xi = a$. In attempting to evaluate the integrals of this type numerically, the presence of the singularity created somewhat of a problem.

The second type of integral, although more complex in appearance, does not contain a singularity and thus, is much more amenable to numerical methods. This type is associated with the coefficients B_1 through B_n in Equation (36) and the coefficients A_1 through A_n in Equation (37). It is of the general form:

$$\int_1^2 f(\xi) g(\xi) d\xi.$$

Regarding the first type, it was decided to evaluate those integrals analytically. The most complicated of these is, of course, the one of n th order and its evaluation will be presented as representative of all others. The n th order integral is of the form:

$$\int_1^2 \frac{(\xi - c)^n}{a - \xi} d\xi.$$

Expansion of the numerator, for all values of n , produces polynomials that have coefficients which are determined according to Paschal's Triangle. Ignoring these coefficients for the time being, this expansion shows that the general form of the integral is actually made up of $n+1$ individual integrals as follows:

$$\int_1^2 \frac{\xi^n d\xi}{a - \xi} + \int_1^2 \frac{\xi^{n-1} d\xi}{a - \xi} + \int_1^2 \frac{\xi^{n-2} d\xi}{a - \xi} + \dots + \int_1^2 \frac{d\xi}{a - \xi}$$

From this, it is seen that the original problem of evaluating one integral containing $(\xi - c)^n$ reduces to evaluation of $n+1$ integrals; each containing one term. Fortunately, an analytical expression is available to aid in evaluating the single integrals. Their general expression is of the following form:

$$\int \frac{\xi^n d\xi}{(a + b\xi)^m}$$

where:

$$b = -1$$

$$\text{and } m = 1.$$

The analytical expression used to evaluate these integrals is [2]:

$$\int \frac{\xi^n d\xi}{(a + b\xi)^m} = \frac{1}{b^{n+1}} \left[\sum_{s=0}^n \frac{n!(-a)^s(a + b\xi)^{n-m-s+1}}{(n-s)!s!(n-m-s+1)} \right] \quad (42)$$

except when $n - m - s + 1 = 0$. In that case, the corresponding term in the square brackets is:

$$\frac{n!(-a)^{n-m+1}}{(n-m+1)!(m-1)!} \ln |a + b\xi|.$$

With the aid of these formulas, an integral containing any power of ξ can be evaluated. The expressions for the integrals containing terms up to ξ^9 are shown in Table I.

The second type of integral was evaluated by way of a numerical

TABLE I

Expansions of Integrals of the Form,

$$\int \frac{x^n dx}{a + bx}, \text{ for } 0 \leq n \leq 9$$

$n=0$	$\frac{1}{b} \left[\ln X \right]$
$n=1$	$\frac{1}{b^2} \left[X - a \ln X \right]$
$n=2$	$\frac{1}{b^3} \left[\frac{X^2}{2} - 2aX + a^2 \ln X \right]$
$n=3$	$\frac{1}{b^4} \left[\frac{X^3}{3} - \frac{3aX^2}{2} + 3a^2X - a^3 \ln X \right]$
$n=4$	$\frac{1}{b^5} \left[\frac{X^4}{4} - \frac{4aX^3}{3} + \frac{6a^2X^2}{2} - 4a^3X + a^4 \ln X \right]$
$n=5$	$\frac{1}{b^6} \left[\frac{X^5}{5} - \frac{5aX^4}{4} + \frac{10a^2X^3}{3} - \frac{10a^3X^2}{2} + 5a^4X - a^5 \ln X \right]$
$n=6$	$\frac{1}{b^7} \left[\frac{X^6}{6} - \frac{6aX^5}{5} + \frac{15a^2X^4}{4} - \frac{20a^3X^3}{3} + \frac{15a^4X^2}{2} - 6a^5X + a^6 \ln X \right]$
$n=7$	$\frac{1}{b^8} \left[\frac{X^7}{7} - \frac{7aX^6}{6} + \frac{21a^2X^5}{5} - \frac{35a^3X^4}{4} + \frac{35a^4X^3}{3} - \frac{21a^5X^2}{2} + 7a^6X - a^7 \ln X \right]$
$n=8$	$\frac{1}{b^9} \left[\frac{X^8}{8} - \frac{8aX^7}{7} + \frac{28a^2X^6}{6} - \frac{56a^3X^5}{5} + \frac{70a^4X^4}{4} - \frac{56a^5X^3}{3} + \frac{28a^6X^2}{2} - 8a^7X + a^8 \ln X \right]$
$n=9$	$\frac{1}{b^{10}} \left[\frac{X^9}{9} - \frac{9aX^8}{8} + \frac{36a^2X^7}{7} - \frac{84a^3X^6}{6} + \frac{126a^4X^5}{5} - \frac{84a^5X^4}{4} + \frac{36a^6X^3}{3} - \frac{36a^7X^2}{2} + 9a^8X - a^9 \ln X \right]$

Where $X = (a + bx)$

integration method commonly known as the trapezoidal rule. This method is used for functions which are continuous over an interval and involves evaluation of the function at points within the interval. Given the values of the function at the points selected; namely $f_0, f_1, f_2, \dots, f_n$, the trapezoidal rule gives the value of the integral according to the following expression [3]:

$$\int_a^b f(x)dx \approx \left[f_0 + 2f_1 + 2f_2 + \dots + 2f_{n+1} + f_n \right] \frac{\Delta x}{2} \quad (43)$$

where Δx is the spacing between evaluation points.

The two procedures described above provide all the information needed to evaluate integrals encountered in attempting to solve this problem. All that remains is to determine how many integrals there will be. The answer to this question is directly dependent on the order of truncation of the power series used to represent the vorticity functions and the number of integrals increases rapidly with increasing truncation order. It turns out that for truncation at order n , $(2n)^2$ integrals are required. In order to generate these integrals, n separate control points need to be selected.

Control points can be any points on the vortex sheets except their beginning and end points. The use of either of these two points gives rise to integrals which are undefined at either the upper or lower limits of integration. These integrals do not have finite values and, therefore, can not be used in the purely numerical computation procedure used to find the unknown vorticity function coefficients.

III. Numerical Examples

In order to prove the validity of the theory presented in the preceding section, it was decided to perform an actual lift calculation using five control points. This required creation of the FORTRAN computer program contained in Appendix A and the truncation of the assumed power series representations of the vorticity functions at the fifth power. The control points were arbitrarily chosen to be .2, .5, .8, 1.1, and 1.4 and were selected so as to fairly evenly cover the 1.55 unit length of the total airfoil section.

Before beginning discussion of this procedure, it is necessary to first specify the values of the numerical constants which are required. The geometric constants are the same as those discussed earlier and are found in Figure 5. The density and velocity of the free stream were determined according to Mach 0.3 flow at sea level. Thus,

$$\rho = .0023769 \text{ slug/ft}^3$$

$$\text{and } V_{\infty} = 334.8 \text{ ft/sec}$$

The values of the sink and source strengths were determined by considering the two-dimensional area rate of flow incident on a line located between the vortex sheets and perpendicular to the direction of the free stream. This area rate of flow is:

$$\dot{A} = (y_1 - y_2) V_{\infty} \quad (44)$$

and carries the units of ft^2/sec . The sink strength was arbitrarily set at $0.7\dot{A}$. For the source, it was decided that its strength should be six times greater than that of the sink. The value of the source strength also included the mass which was "lost" into the sink and was determined according to the following formula:

$$\Gamma_{\text{source}} = \Gamma_{\text{sink}} + 6 \Gamma_{\text{sink}} \quad (45)$$

The reason for adding the sink strength to that of the source was caused by the need to "regain" the flow which was absorbed by the sink. In reality, this flow is associated with the free stream and represents the air which passes through the wing slots. The reason for using the factor of six in the other source term was to account for the substantial mass addition to the slot flow caused by the ejector. The results of these calculations are:

$$\dot{L}_{\text{sink}} = 35.1540 \text{ ft}^2/\text{sec}$$

$$\dot{L}_{\text{source}} = 246.078 \text{ ft}^2/\text{sec}$$

In order to generate the system of equations needed to solve the problem as posed, Equations (36) and (37) with fifth order truncations are used. These equations become:

$$\begin{aligned} A_1 \int_0^c \frac{\xi_1 - c}{x - \xi_1} d\xi_1 + A_2 \int_0^c \frac{(\xi_1 - c)^2}{x - \xi_1} d\xi_1 + A_3 \int_0^c \frac{(\xi_1 - c)^3}{x - \xi_1} d\xi_1 + A_4 \int_0^c \frac{(\xi_1 - c)^4}{x - \xi_1} d\xi_1 + A_5 \int_0^c \frac{(\xi_1 - c)^5}{x - \xi_1} d\xi_1 + \\ B_1 \int_0^l (\xi_2 - l) \Delta d\xi_2 + B_2 \int_0^l (\xi_2 - l)^2 \Delta d\xi_2 + B_3 \int_0^l (\xi_2 - l)^3 \Delta d\xi_2 + \\ B_4 \int_0^l (\xi_2 - l)^4 \Delta d\xi_2 + B_5 \int_0^l (\xi_2 - l)^5 \Delta d\xi_2 = N_{\text{upper}} \end{aligned} \quad (46)$$

$$\begin{aligned} A_1 \int_0^c (\xi_1 - c) \theta d\xi_1 + A_2 \int_0^c (\xi_1 - c)^2 \theta d\xi_1 + A_3 \int_0^c (\xi_1 - c)^3 \theta d\xi_1 + A_4 \int_0^c (\xi_1 - c)^4 \theta d\xi_1 + \\ A_5 \int_0^c (\xi_1 - c)^5 \theta d\xi_1 + B_1 \int_0^l \frac{\xi_2 - l}{x - x_3 - \xi_2} d\xi_2 + B_2 \int_0^l \frac{(\xi_2 - l)^2}{x - x_3 - \xi_2} d\xi_2 + B_3 \int_0^l \frac{(\xi_2 - l)^3}{x - x_3 - \xi_2} d\xi_2 + \\ B_4 \int_0^l \frac{(\xi_2 - l)^4}{x - x_3 - \xi_2} d\xi_2 + B_5 \int_0^l \frac{(\xi_2 - l)^5}{x - x_3 - \xi_2} d\xi_2 = N_{\text{lower}} \end{aligned} \quad (47)$$

In order to determine unique values for A_1 through A_5 and B_1 through B_5 , each of these equations was evaluated for the five different values of x corresponding to the control points selected. For example, for the first control point, $x = 0.2$, the two equations became:

$$\begin{aligned}
& A_1 \int_0^c \frac{\xi_1 - c}{.2 - \xi_1} d\xi_1 + A_2 \int_0^c \frac{(\xi_1 - c)^2}{.2 - \xi_1} d\xi_1 + A_3 \int_0^c \frac{(\xi_1 - c)^3}{.2 - \xi_1} d\xi_1 + A_4 \int_0^c \frac{(\xi_1 - c)^4}{.2 - \xi_1} d\xi_1 + \\
& A_5 \int_0^c \frac{(\xi_1 - c)^5}{.2 - \xi_1} d\xi_1 + B_1 \int_0^l (\xi_2 - l) \Delta d\xi_2 + B_2 \int_0^l (\xi_2 - l)^2 \Delta d\xi_2 + \\
& B_3 \int_0^l (\xi_2 - l)^3 \Delta d\xi_2 + B_4 \int_0^l (\xi_2 - l)^4 \Delta d\xi_2 + \\
& B_5 \int_0^l (\xi_2 - l)^5 \Delta d\xi_2 = N_{upper}
\end{aligned} \tag{48}$$

$$\begin{aligned}
& A_1 \int_0^c (\xi_1 - c) \theta d\xi_1 + A_2 \int_0^c (\xi_1 - c)^2 \theta d\xi_1 + A_3 \int_0^c (\xi_1 - c)^3 \theta d\xi_1 + A_4 \int_0^c (\xi_1 - c)^4 \theta d\xi_1 + \\
& A_5 \int_0^c (\xi_1 - c)^5 \theta d\xi_1 + B_1 \int_0^l \frac{\xi_2 - l}{.2 - \xi_3 - \xi_2} d\xi_2 + B_2 \int_0^l \frac{(\xi_2 - l)^2}{.2 - \xi_3 - \xi_2} d\xi_2 + \\
& B_3 \int_0^l \frac{(\xi_2 - l)^3}{.2 - \xi_3 - \xi_2} d\xi_2 + B_4 \int_0^l \frac{(\xi_2 - l)^4}{.2 - \xi_3 - \xi_2} d\xi_2 + \\
& B_5 \int_0^l \frac{(\xi_2 - l)^5}{.2 - \xi_3 - \xi_2} d\xi_2 = N_{lower}
\end{aligned} \tag{49}$$

Similar equations were generated for the four other control points by replacing the constant 0.2 by, successively, 0.5, 0.8, 1.1, and 1.4. From these 10 equations, 100 different integrals result. For example, for the A_1 coefficient, the integrals are:

$$U_{1,1} = \int_0^c \frac{\xi_1 - c}{.2 - \xi_1} d\xi_1, \tag{50}$$

$$U_{2,1} = \int_0^c \frac{\xi_1 - c}{.5 - \xi_1} d\xi_1, \tag{51}$$

$$U_{3,1} = \int_0^c \frac{\xi_1 - c}{.8 - \xi_1} d\xi_1, \tag{52}$$

$$U_{4,1} = \int_0^c \frac{\xi_1 - c}{1.1 - \xi_1} d\xi_1, \tag{53}$$

$$U_{5,1} = \int_0^c \frac{\xi_1 - c}{1.4 - \xi_1} d\xi_1, \tag{54}$$

$$U_{6,1} = \int_0^c \frac{(\xi_1 - c) \cos \left(\tan^{-1} \frac{y_1 - y_2}{.2 - \xi_1} \right)}{\sqrt{(.2 - \xi_1)^2 + (y_1 - y_2)^2}} d\xi_1, \tag{55}$$

$$U_{7,1} = \int_0^c \frac{(\xi_1 - c) \cos(\tan^{-1} \frac{y_1 - y_2}{.5 - \xi_1})}{\sqrt{(.5 - \xi_1)^2 + (y_1 - y_2)^2}} d\xi_1 \quad (56)$$

$$U_{8,1} = \int_0^c \frac{(\xi_1 - c) \cos(\tan^{-1} \frac{y_1 - y_2}{.8 - \xi_1})}{\sqrt{(.8 - \xi_1)^2 + (y_1 - y_2)^2}} d\xi_1 \quad (57)$$

$$U_{9,1} = \int_0^c \frac{(\xi_1 - c) \cos(\tan^{-1} \frac{y_1 - y_2}{1.1 - \xi_1})}{\sqrt{(1.1 - \xi_1)^2 + (y_1 - y_2)^2}} d\xi_1 \quad (58)$$

$$U_{10,1} = \int_0^c \frac{(\xi_1 - c) \cos(\tan^{-1} \frac{y_1 - y_2}{1.4 - \xi_1})}{\sqrt{(1.4 - \xi_1)^2 + (y_1 - y_2)^2}} d\xi_1 \quad (59)$$

The values of these integrals comprise the first column of the U matrix. Similarly, the integrals associated with the B₅ coefficient make up the tenth column of the matrix. They are:

$$U_{1,10} = \int_0^l \frac{(\xi_2 - l)^5 \cos(\tan^{-1} \frac{y_1 - y_2}{.2 - X_3 - \xi_2})}{\sqrt{(.2 - X_3 - \xi_2)^2 + (y_1 - y_2)^2}} d\xi_2 \quad (60)$$

$$U_{2,10} = \int_0^l \frac{(\xi_2 - l)^5 \cos(\tan^{-1} \frac{y_1 - y_2}{.5 - X_3 - \xi_2})}{\sqrt{(.5 - X_3 - \xi_2)^2 + (y_1 - y_2)^2}} d\xi_2 \quad (61)$$

$$U_{3,10} = \int_0^l \frac{(\xi_2 - l)^5 \cos(\tan^{-1} \frac{y_1 - y_2}{.8 - X_3 - \xi_2})}{\sqrt{(.8 - X_3 - \xi_2)^2 + (y_1 - y_2)^2}} d\xi_2 \quad (62)$$

$$U_{4,10} = \int_0^l \frac{(\xi_2 - l)^5 \cos(\tan^{-1} \frac{y_1 - y_2}{1.1 - X_3 - \xi_2})}{\sqrt{(1.1 - X_3 - \xi_2)^2 + (y_1 - y_2)^2}} d\xi_2 \quad (63)$$

$$U_{5,10} = \int_0^l \frac{(\xi_2 - l)^5 \cos(\tan^{-1} \frac{y_1 - y_2}{1.4 - x_3 - \xi_2})}{\sqrt{(1.4 - x_3 - \xi_2)^2 + (y_1 - y_2)^2}} d\xi_2 \quad (64)$$

$$U_{6,10} = \int_0^l \frac{(\xi_2 - l)^5}{.2 - x_3 - \xi_2} d\xi_2 \quad (65)$$

$$U_{7,10} = \int_0^l \frac{(\xi_2 - l)^5}{.5 - x_3 - \xi_2} d\xi_2 \quad (66)$$

$$U_{8,10} = \int_0^l \frac{(\xi_2 - l)^5}{.8 - x_3 - \xi_2} d\xi_2 \quad (67)$$

$$U_{9,10} = \int_0^l \frac{(\xi_2 - l)^5}{1.1 - x_3 - \xi_2} d\xi_2 \quad (68)$$

$$U_{10,10} = \int_0^l \frac{(\xi_2 - l)^5}{1.4 - x_3 - \xi_2} d\xi_2 \quad (69)$$

The other 80 integrals are defined in similar fashion for the other coefficients, but they will not be listed here. It is sufficient to say that the U matrix which results from these integrals is 10 by 10 in size and can easily be inverted by existing routines (3).

The values of N_{upper} and N_{lower} were calculated for the five different control points from Equations (33) and (34). These constants comprise the N vector in Equation (39). From Equation (40), values for the unknown coefficients were determined to be:

$$A_1 = -130782.2$$

$$A_2 = -4213634.4$$

$$A_3 = -20230426.5$$

$$A_4 = -32400910.7$$

$$A_5 = -16521998.5$$

$$B_1 = -45936.3$$

$$B_2 = 545461.9$$

$$B_3 = 4372389.1$$

$$B_4 = 8572411.4$$

$$B_5 = 4925628.4$$

These coefficients give rise to vorticity functions that cause the y-components of velocity at the control points to be zero. The lift per unit span is calculated from these functions according to Equation (41) and is:

$$L' = -2230.5 \text{ lbf/ft.}$$

The negative sign associated with this value, needless to say, looks bad and casts doubt on the validity of the procedure used. However, inspection of Figures 8 through 11 shows that the boundary and auxiliary conditions have been satisfied. Namely, the y-components of velocity are zero at the control points and both $\gamma_1(\xi_1)$ and $\gamma_2(\xi_2)$ are zero at the trailing edges of the vortex sheets. Thus, in spite of the seemingly wrong answer for L' , it appears that the model and theory are correct and that the computer program performs as expected. As a step toward investigating potential reasons why negative lift was obtained, the calculations were repeated for different selections of control points. The results obtained are summarized in Table II.

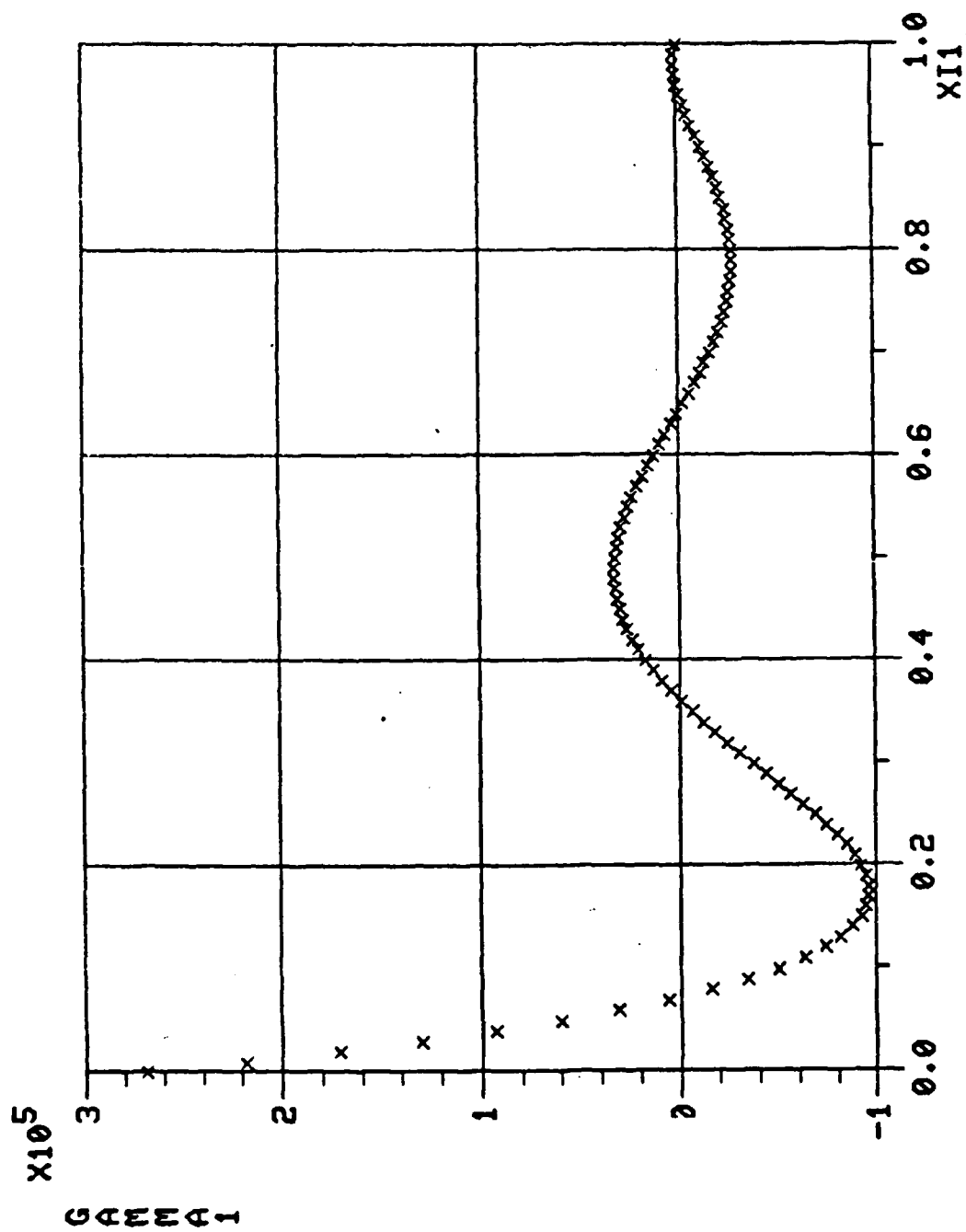


Figure 8. Upper Vorticity Distribution for Control Points: 0.2, 0.5, 0.8, 1.1, 1.4

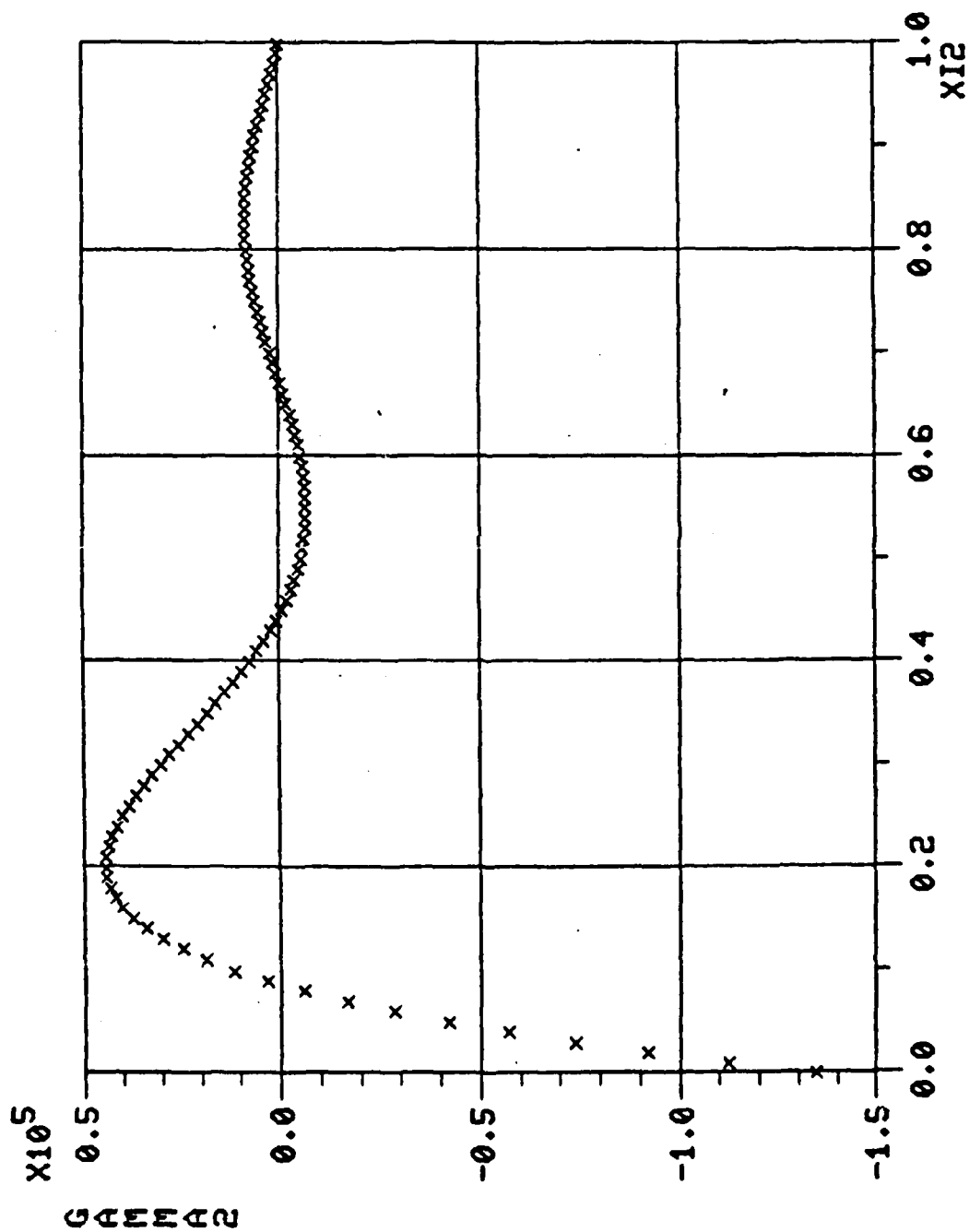


Figure 9. Lower Vorticity Distribution for Control Points: 0.2, 0.5, 0.8, 1.1, 1.4

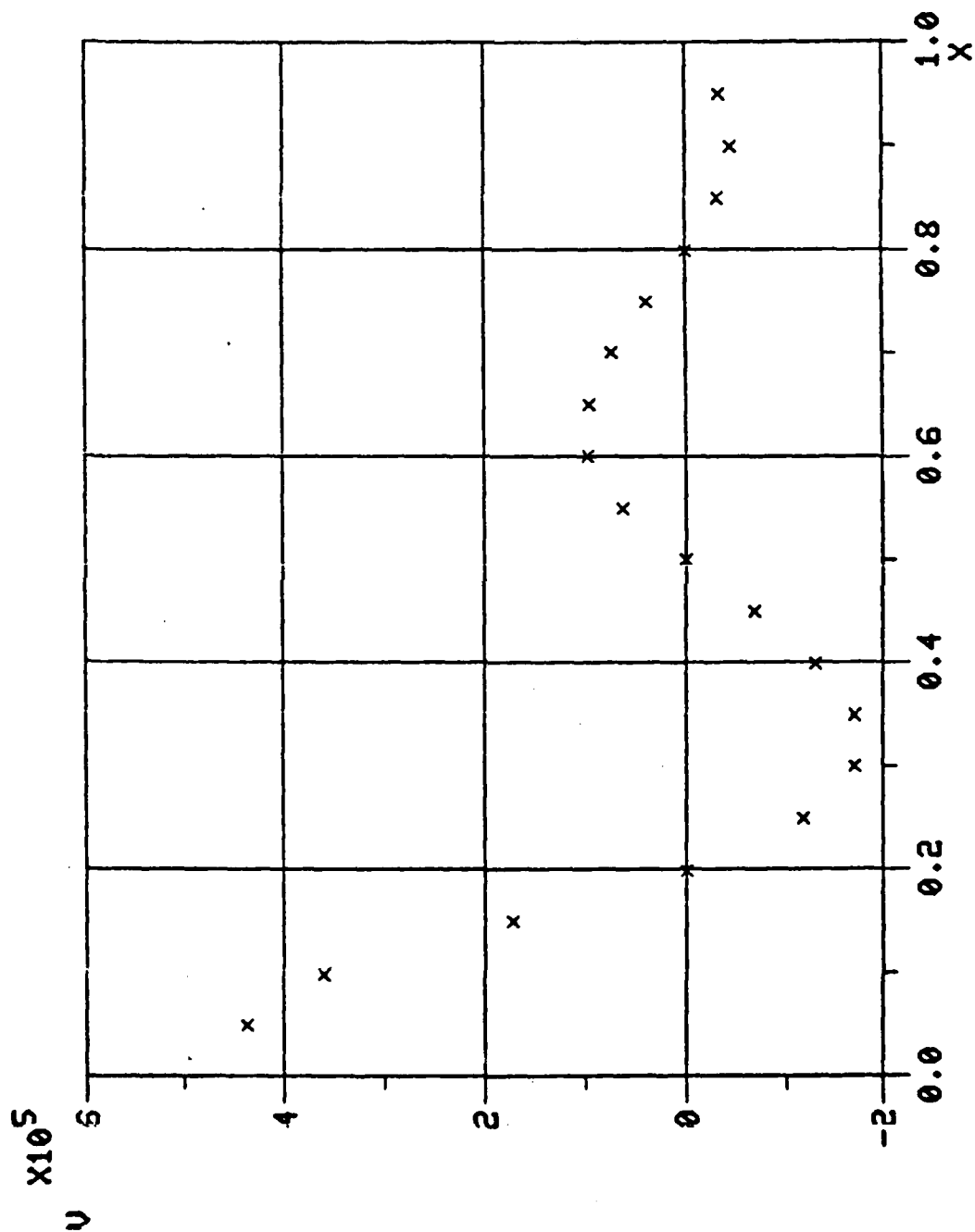


Figure 10. Y-Components of Velocity over Upper Sheet for Control Points: 0.2, 0.5, 0.8, 1.1, 1.4

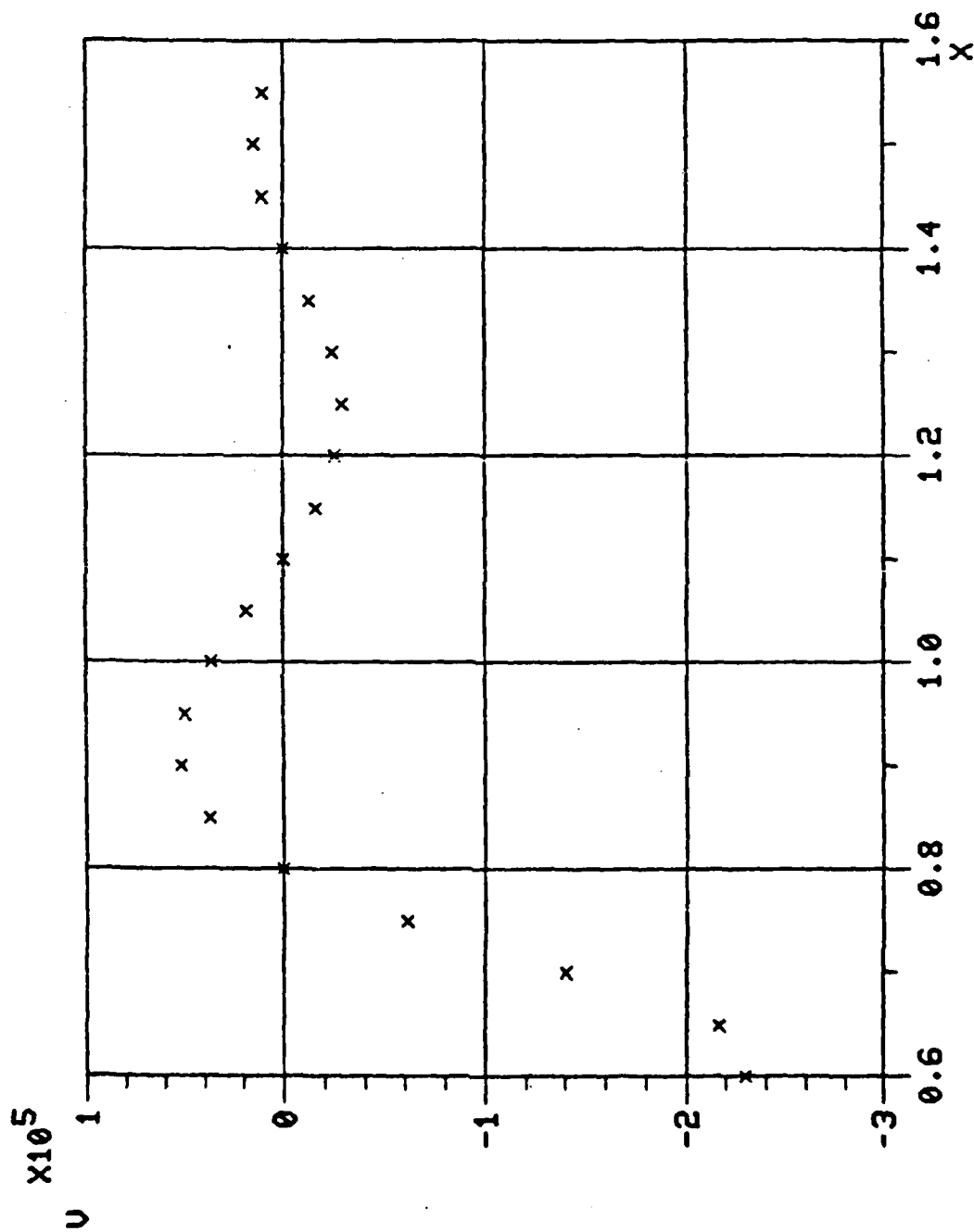


Figure 11. Y-Components of Velocity over Lower Sheet for Control Points:
0.2, 0.5, 0.8, 1.1, 1.4

TABLE II

Lift Calculations Resulting from Four Different Control
Point Selections for Fifth Order Truncations

<u>Control Points</u>	<u>Lift per Unit Span</u>
.2, .5, .8, 1.1, 1.4	-2230.5 lbf/ft
.1, .45, .80, 1.15, 1.50	3690.1 lbf/ft
.05, .40, .75, 1.10, 1.45	-289.3 lbf/ft
.1, .3, .5, .7, .9	343.8 lbf/ft

From Table II, it is apparent that the lift is directly related to the control points used. Of course, there are an infinite number of possible control point selections and the criterion by which the "correct" ones could be determined is unknown. Further, since the choice of control points was arbitrary, their selection should not have an impact on the final answer. However, the consistency with which the boundary and auxiliary conditions were satisfied does appear to indicate that the solution method, itself, is valid (See Figures 12 through 23).

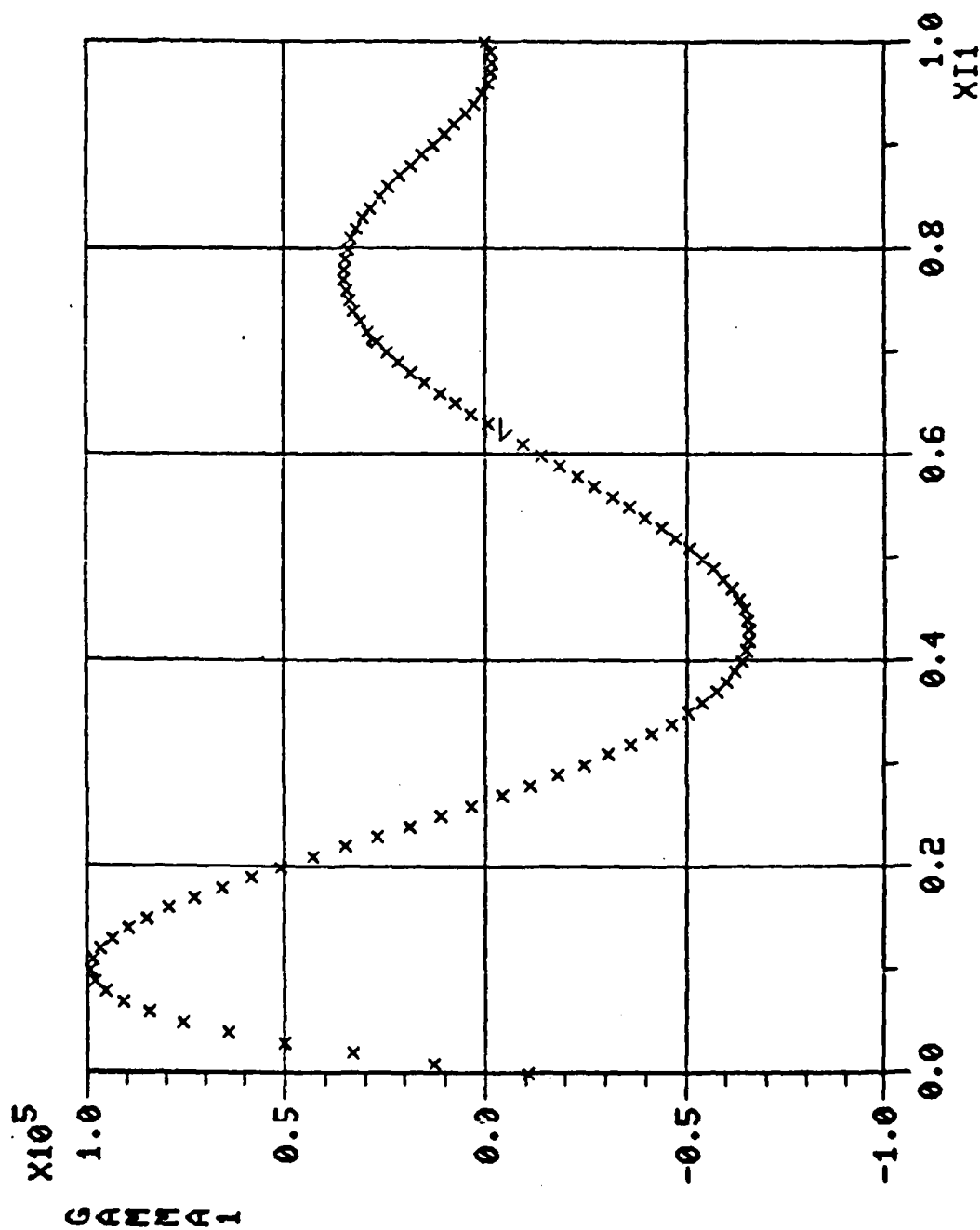


Figure 12. Upper Vorticity Distribution for Control Points: .10, .45, .80, 1.15, 1.50

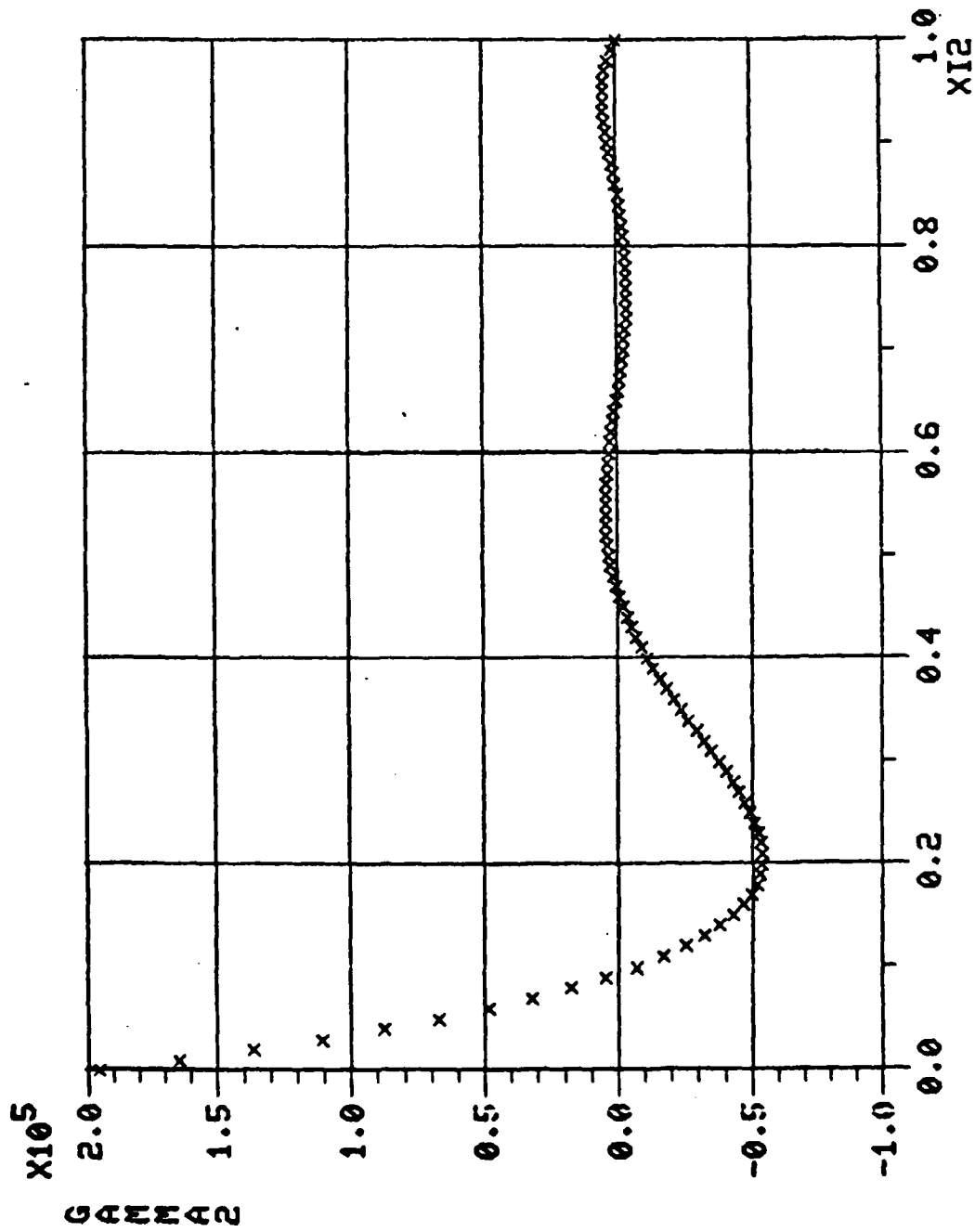


Figure 13. Lower Vorticity Distribution for Control Points: .10, .45, .80, 1.15, 1.50

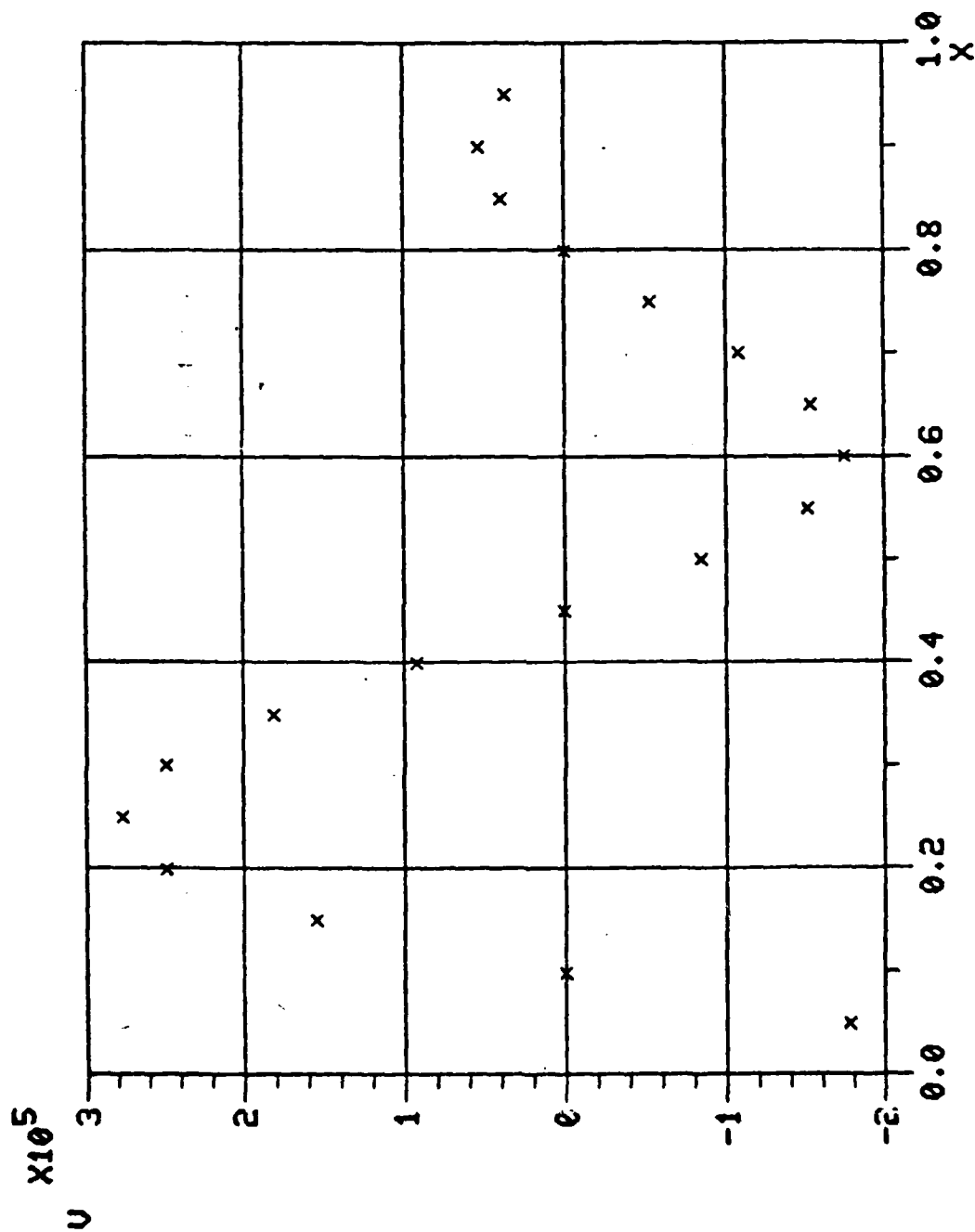


Figure 14. Y-Components of Velocity over Upper Sheet for Control Points: .10, .45, .80, 1.15, 1.50

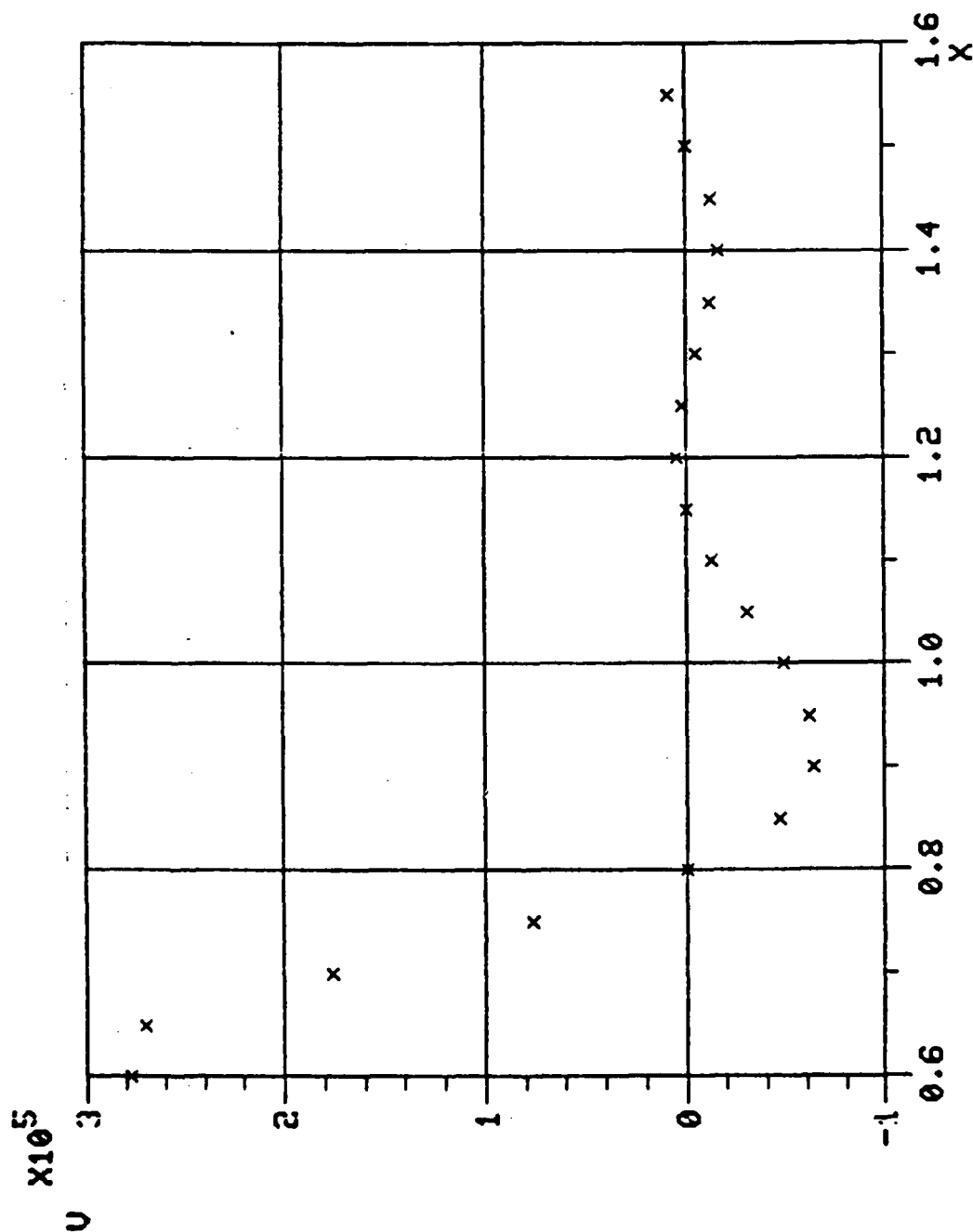


Figure 15. Y-Components of Velocity over Lower Sheet for Control Points:
.10, .45, .80, 1.15, 1.50

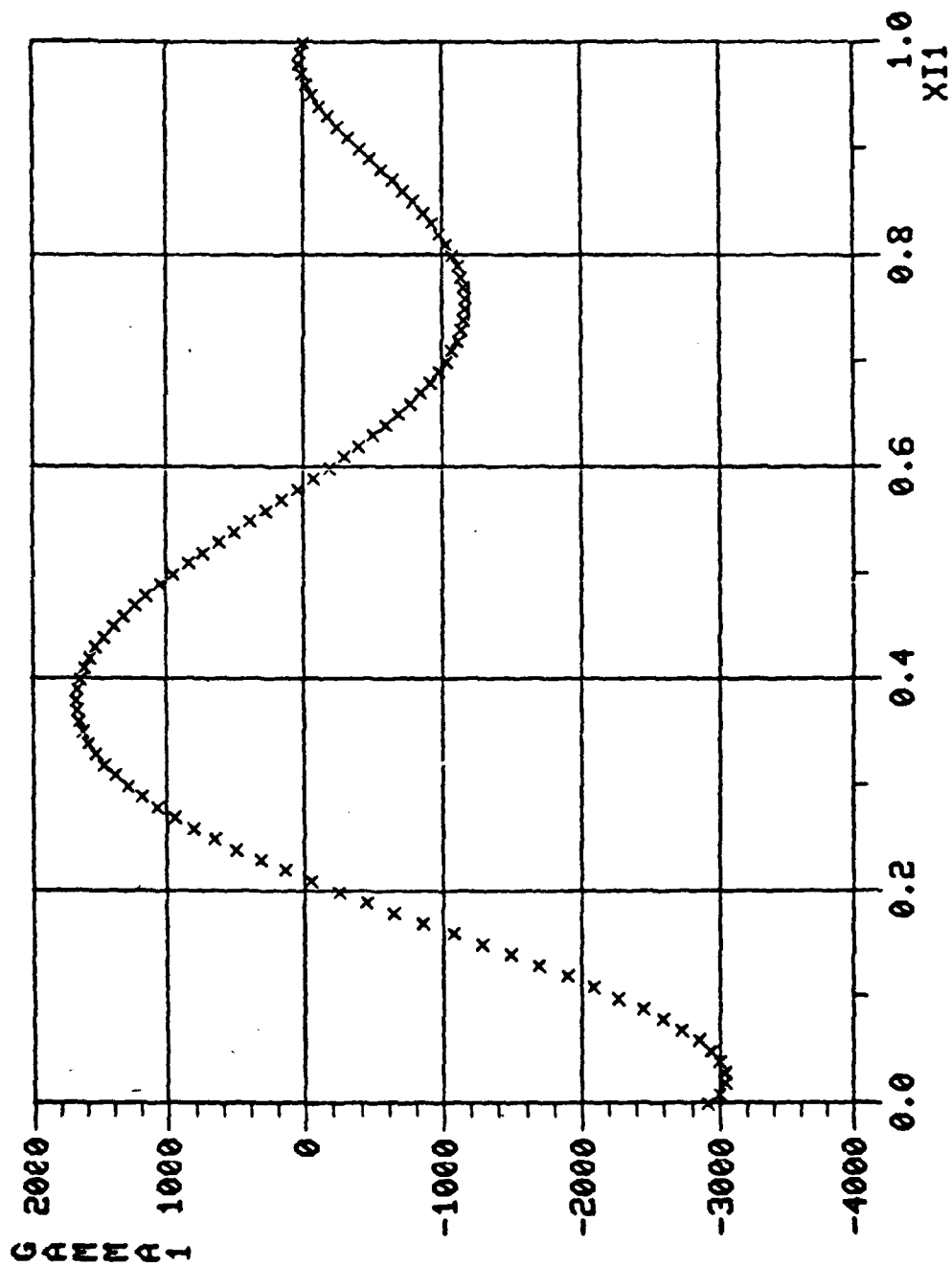


Figure 16. Upper Vorticity Distribution for Control Points: .05, .40, .75, 1.10, 1.45

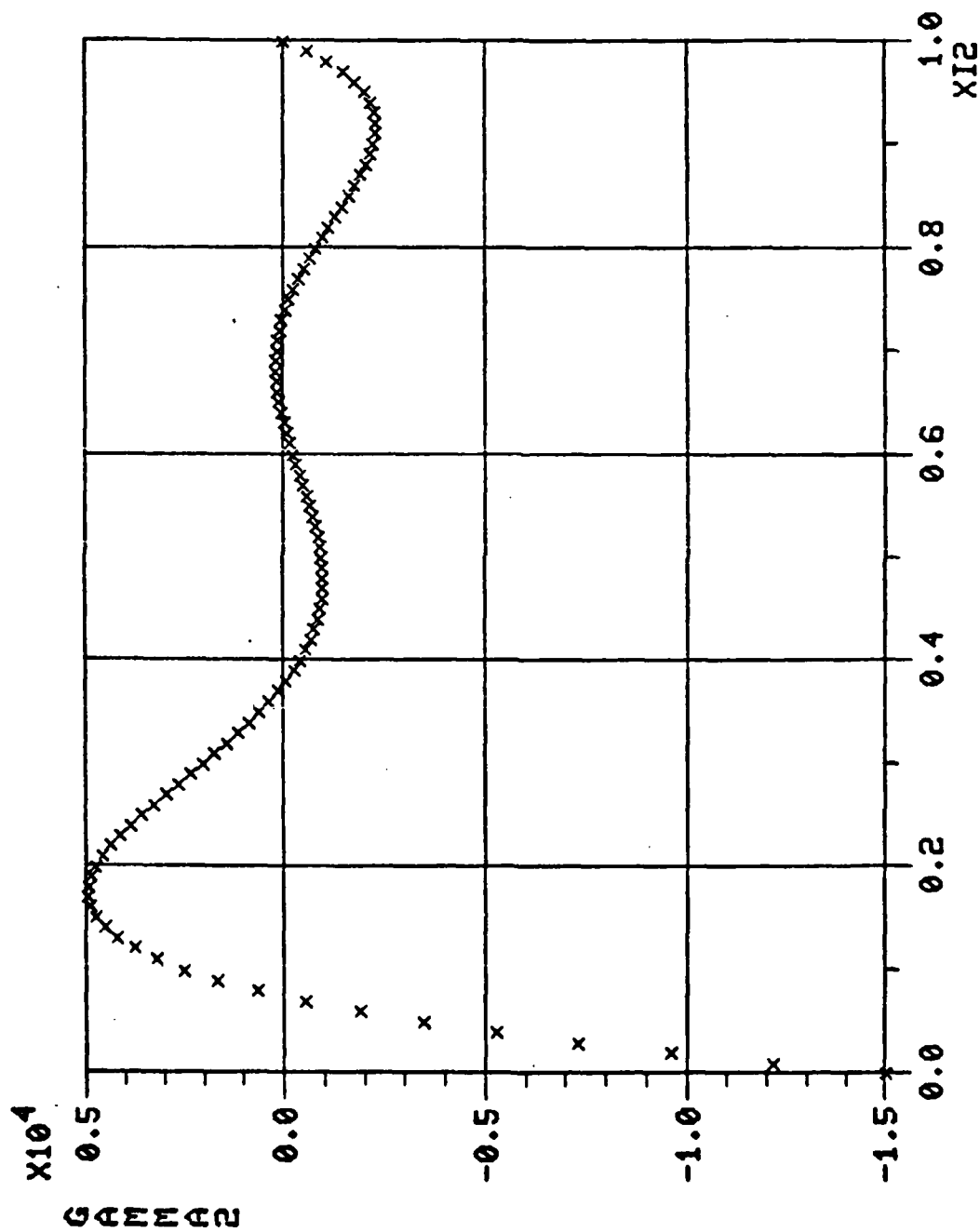


Figure 17. Lower Vorticity Distribution for Control Points: .05, .40, .75, 1.10, 1.45

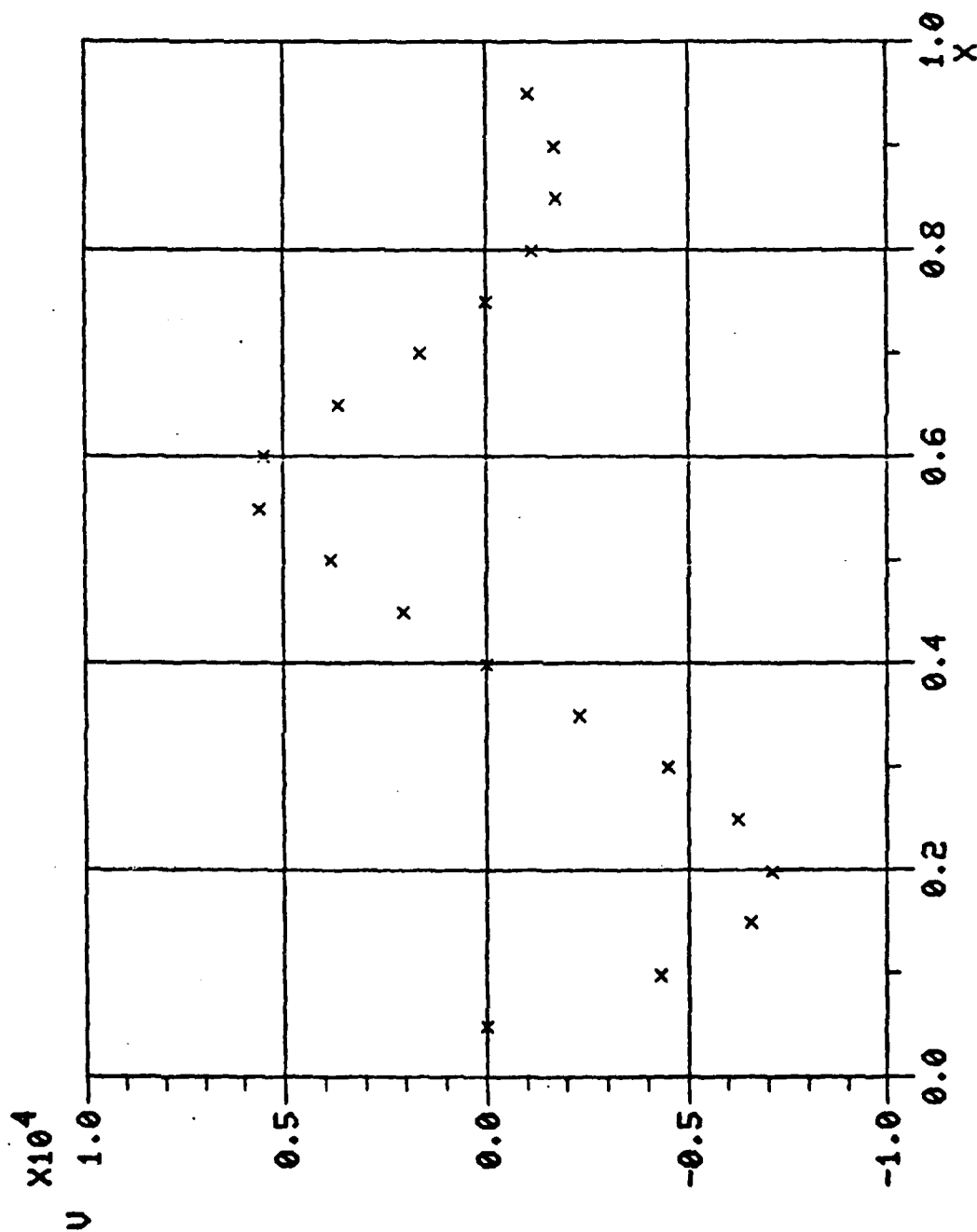


Figure 18. Y-Components of Velocity over Upper Sheet for Control Points: 0.5, .40, .75, 1.10, 1.45

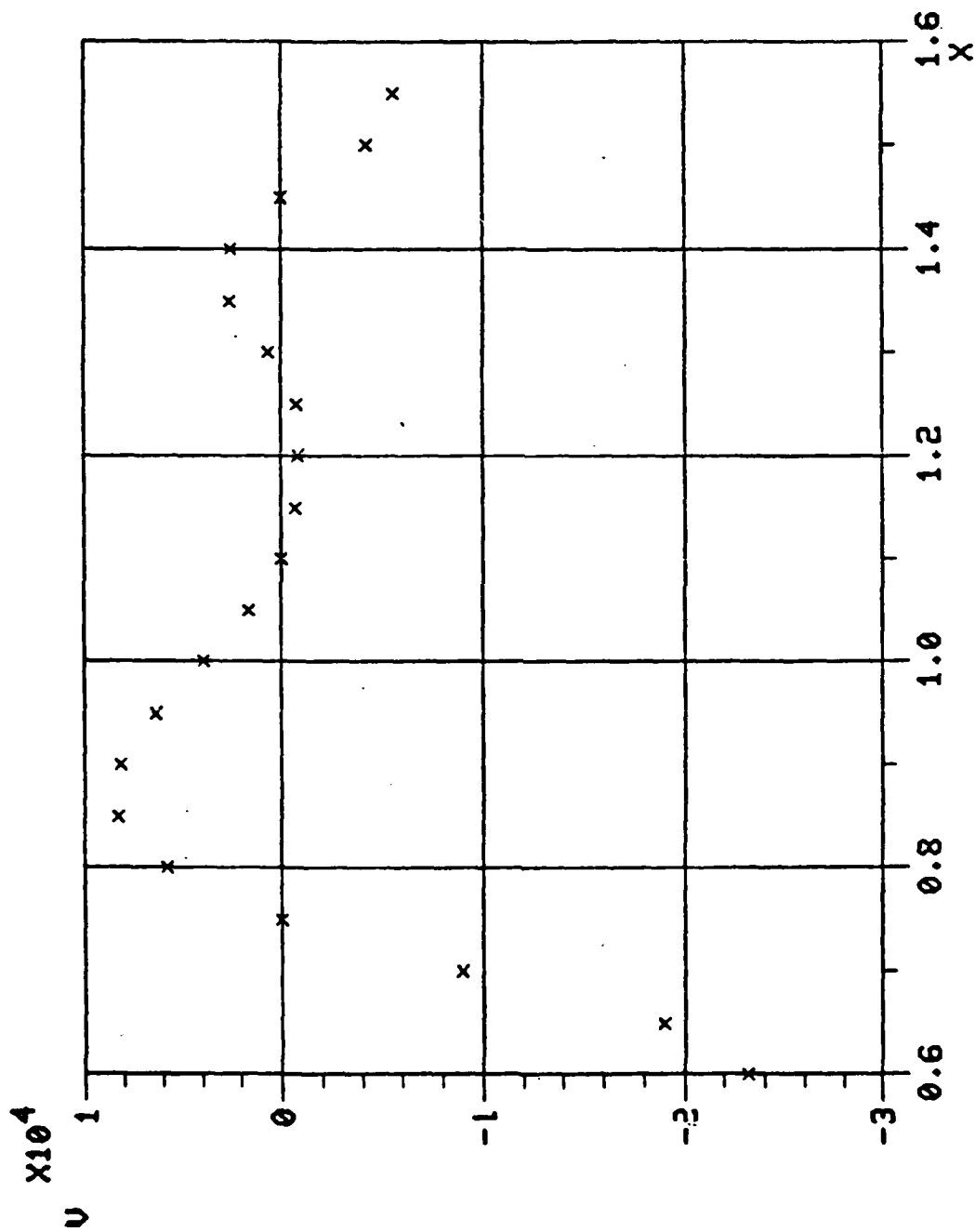


Figure 19. Y-Components of Velocity over Lower Sheet for Control Points:
.05, .40, .75, 1.10, 1.45

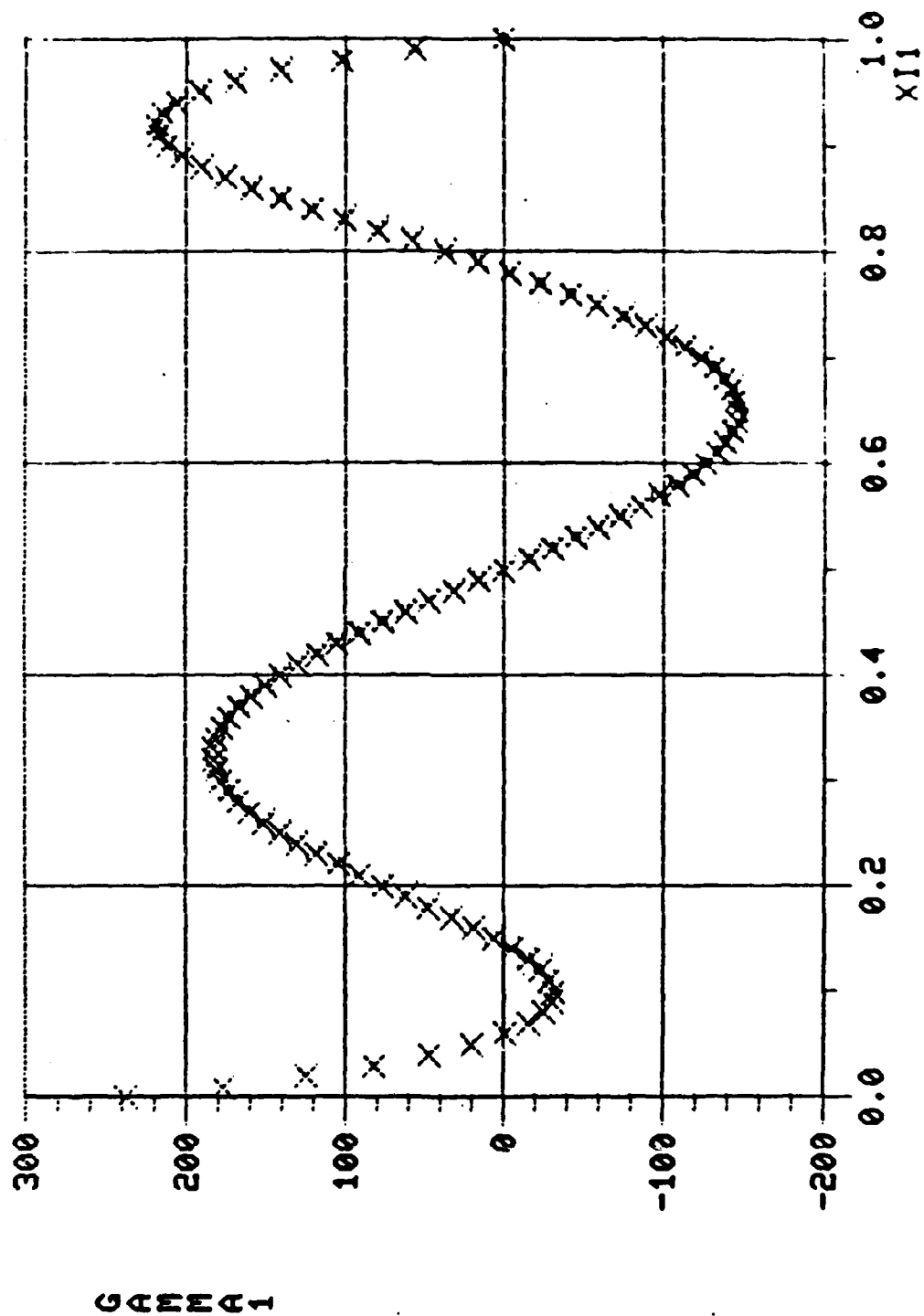


Figure 20. Upper Vorticity Distribution for Control Points: .10, .30, .50, .70, .90

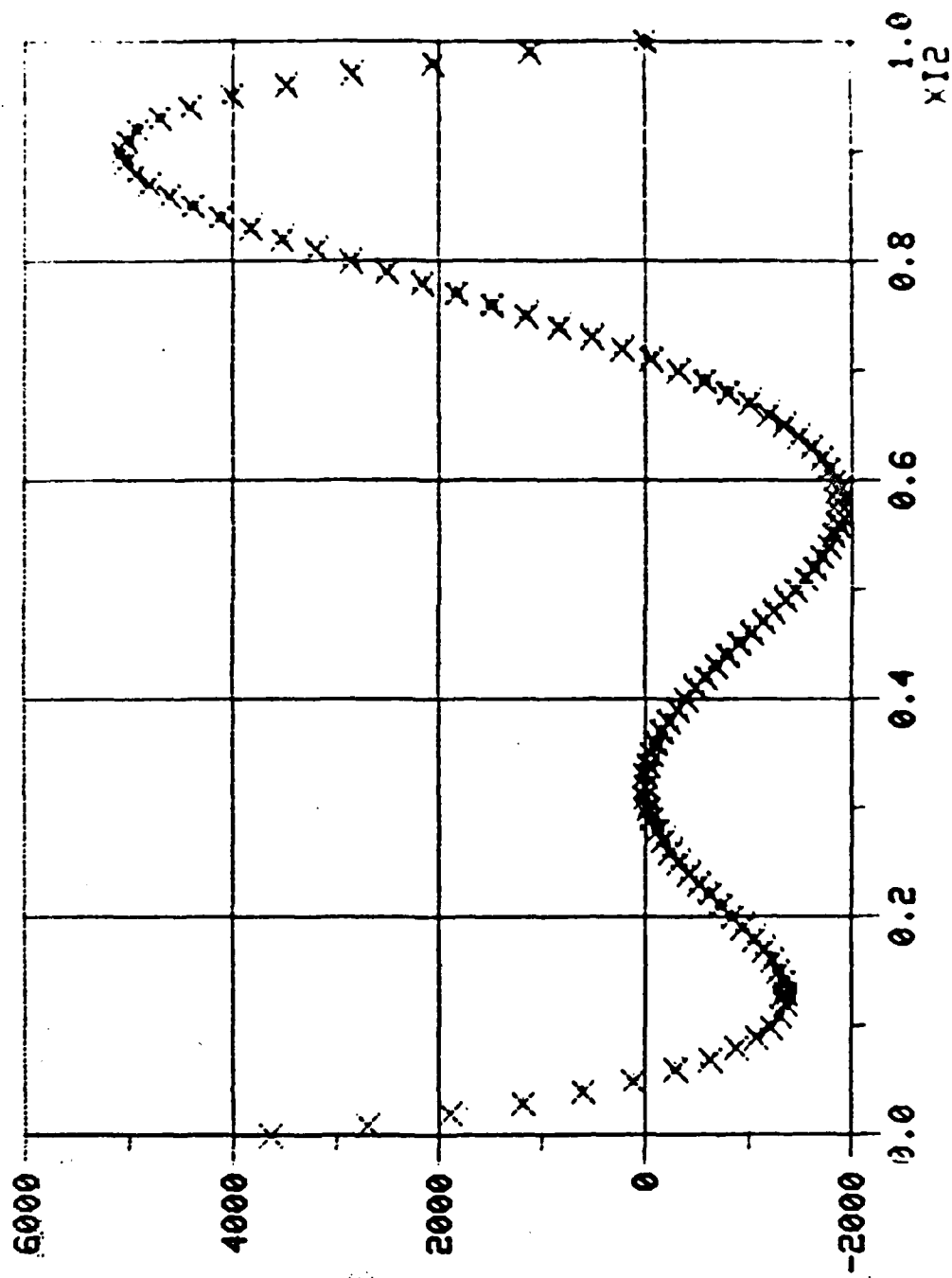


Figure 21. Lower Vorticity Distribution for Control Points: .10, .30, .50, .70, .90

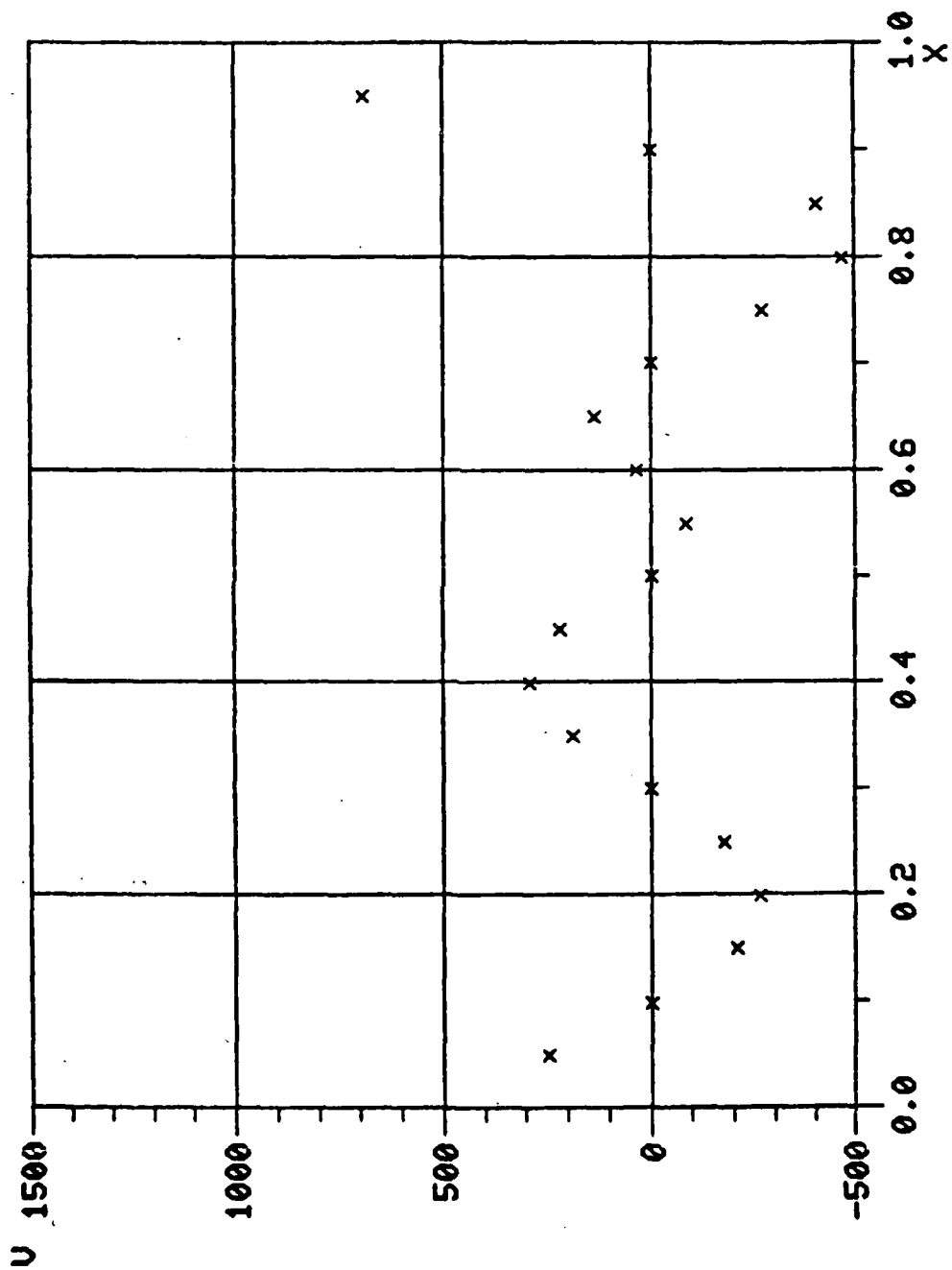


Figure 22. Y-Components of Velocity over Upper Sheet for Control Points:
.10, .30, .50, .70, .90

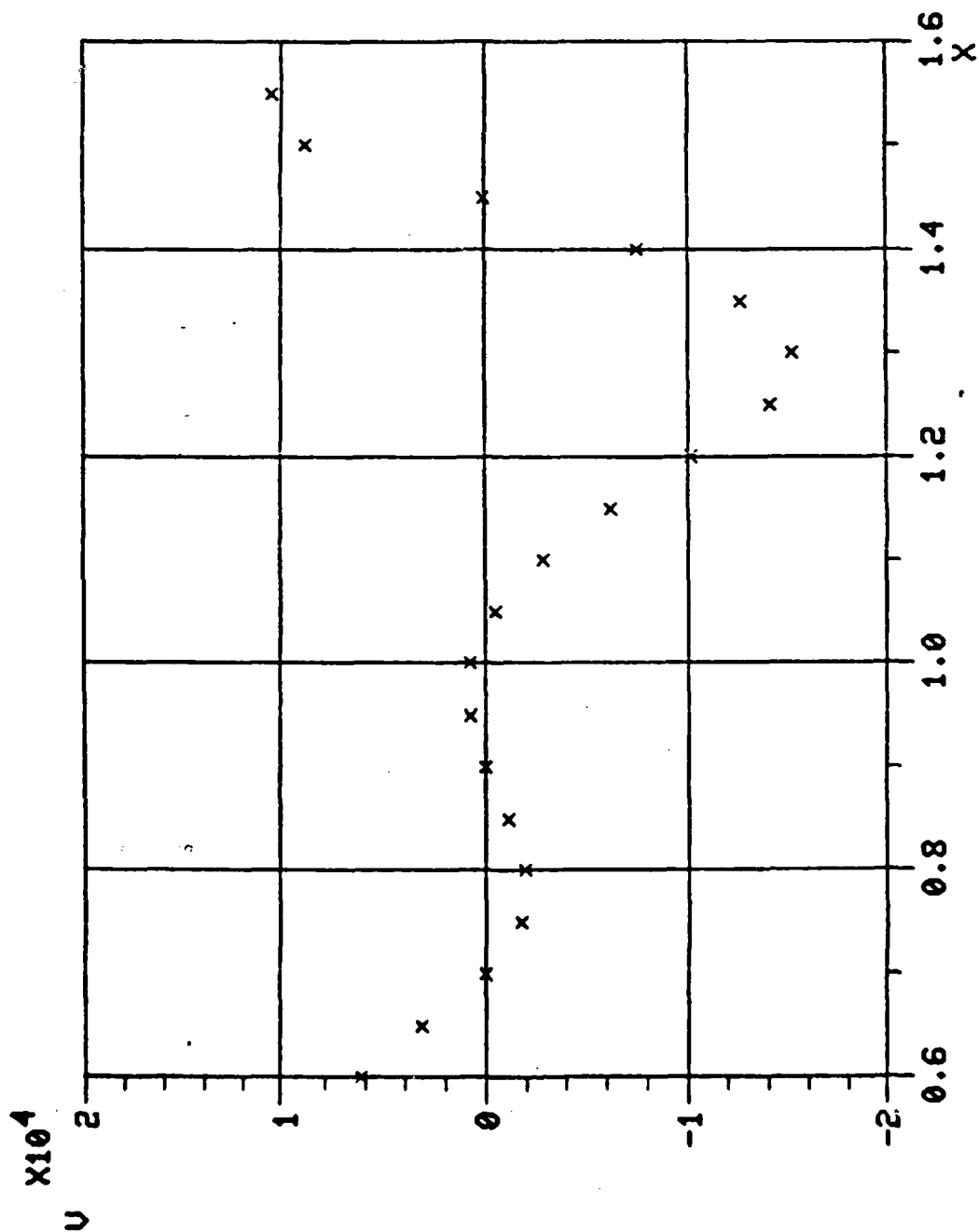


Figure 23. Y-Components of Velocity over Lower Sheet for Control Points: .10, .30, .50, .70, .90

IV. Conclusions

A conclusion that can be drawn from consideration of the numerical examples is that more than five control points are needed for determination of the lift. It has been shown that the flow tangency boundary condition is satisfied at the control points, but it is not satisfied at other points on the sheets. It is believed the validity of the lift calculated from the model is directly dependent on how well the sheets are made to coincide with streamlines of the flow field. From inspection of the plots of the y-components of velocity over the sheets, it is apparent that for the five-control-point case, the sheets do not closely resemble streamlines.

By using more control points, the flow tangency requirement would be satisfied at more points on the sheets and, as a result, they would more closely resemble the streamlines. Use of more control points will entail much more work, however. This work will not be theoretical in nature, but rather, will involve the fairly tedious procedure of determining values for the definite integrals,

$$\int_1^2 \frac{\xi^n d\xi}{a-\xi}$$

where n takes on values from zero to a very high integer.

V. Recommendations

Inspection of Table I shows that the series which result from the integrals of concern are not built one upon the other -- i.e., by simply adding a new term to a previous string of terms. It is seen that the coefficients for any term containing $(a + b\xi)$ to any power change as n changes. This lack of simplicity in the generation of these series complicates the manner in which they could be developed by a computer. If these series and the associated integrals are worked out by hand, the large number of terms involved can soon become overwhelming. For example, an integral containing only a fifth order polynomial gives rise to six individual integrals containing the following terms: x^5 , x^4 , x^3 , x^2 , x^1 , and x^0 . These integrals contain, respectively, six, five, four, three, two, and one term and, the original integral requires the summation of these terms -- i.e., 21 -- for its evaluation. Clearly, it can be seen that to do this procedure by hand would be very laborious.

The most promising method for solution of this problem appears to involve creation of a computer routine based on Equation (42) which would generate the series representations of the integrals for any value of n . If such a routine were available, many more than five control points could be used and thus, the vortex sheets could be brought more into line with the flow field streamlines. Then, the calculated values of L' probably would not display the same erratic behavior as they have done for the cases where only five control points were used.

Bibliography

1. Bertin, J. J. and M. L. Smith, Aerodynamics for Engineers, Prentice-Hall, Inc., Englewood Cliffs, New Jersey, 1979.
2. Dwight, H. B., Tables of Integrals and Other Mathematical Data, The Macmillan Company, New York, New York, 1947.
3. Hornbeck, R. W., Numerical Methods, Quantum Publishers, Inc., New York, New York, 1975.
4. Kuethe, A. M. and C. Y. Chow, Foundations of Aerodynamics, John Wiley & Sons, New York, New York, 1976,
5. Nagaraga, K. S., conversations with author at Air Force Wright Aeronautical Laboratory, 1981.
6. Purcell, E. J., Calculus with Analytic Geometry, Meredith Publishing Co., New York, New York, 1965.
7. Squyers, R., K. Nagaraga, J. Porter, and G. Cudahy, "Ejector Powered Propulsive and High Lift Subsonic Wing."
8. Vought Corporation Advanced Technology Center, "Ejector Wing Design Status Report, 17 August 1979 to 17 September 1979," ATC Report No. R-9100/9CR-49, September 1979.
9. Woolard, H. W., "Thin-Airfoil Theory of an Ejector-Flapped Wing Section," Journal of Aircraft, Vol. 12, No. 1, January 1975, pp. 26-33.

APPENDIX A

Listed on the following 11 pages is the computer program that was used to make the lift calculation. The inputs to the program are contained in lines 17 through 39 and consist of the required geometric values and aerodynamic constants. Evaluation of integrals is done in lines 44 through 252, and the sink- and source-related constants are generated in lines 260 through 273. Following these calculations, the U matrix is inverted by means of the subroutine labeled INVDET.

Output from the program begins with line 315 which prints out values of the upper vorticity distribution. Similarly, line 344 prints out values of the lower vorticity distribution. The overall lift per unit span is output via line 364.

The program also contains a large section which verifies that the flow tangency condition is, indeed, satisfied. Velocities and pressures at points along the upper sheet are output via line 459 and similar values for the lower sheet are output via line 538.

The plots included in this report were not generated by this program, but were made via a separate plotting program. Potential users of this program are advised to procure similar independent plotting routines if graphical output is desired.

```

D=SDNW*WORK(1),FINAL
1  PROGRAM THMOD3
2  REAL U(10,10),N(10),AB(10)
3  REAL LIFT,L1,L2,HLIFT,INCL1,INCL2
4  REAL LBROT,INCBOT
5  REAL LBTOP,INCTOP
6  REAL P1(20),P2(20),P3(20),P4(20),VTOP(20)
7  REAL P5(20),P6(20),P7(20),P8(20),VBOT(20)
8  REAL P9(20),P10(20),P11(20),UTOP(20)
9  REAL P12(20),P13(20),P14(20),UBOT(20)
10 REAL PTOP(20),PBOT(20)
11 INTEGER STEPL
12 C
13 C
14 C
15 C
16 C
17 C
18 C
19 C
20 C
21 C
22 C
23 C
24 C
25 C
26 C
27 10 FORMAT(' THE VALUES OF C X1 X2 X3 X4 Y1 Y2 ARE: '//)
28 WRITE(6,'(1X,7F14.9)') C,X1,X2,X3,X4,Y1,Y2
29 C
30 C
31 C
32 C
33 C
34 C
35 C
36 C
37 C
38 C
39 C
40 C
41 20 FORMAT(' VALUES OF F1,F2,SINK AND SOURCE STRENGTHS ARE: '//)
42 WRITE(6,'(1X,4F16.4)') F1,F2,SINK,SOURCE
43 C
44 C
45 C
46 C
47 C
48 C
49 C
50 C
51 C
52 C
53 C
54 C
55 C
56 C

```

THESE ARE THE GEOMETRIC PARAMETERS OF THE MODEL

C=1.0
X3=.55
X1=X3-.05
BL=1.0
X4=X3+BL
X2=(C+X4)/2.
Y1=.075
Y2=(-1.)*Y1
H=Y1-Y2
WRITE(6,10)

THESE ARE THE AERO PARAMETERS OF THE MODEL

P1=3.14159
RHO=.00237690
VEL=334.8
PRES=2116.22
F1=.7
SINK=H*VEL*F1
F2=.6
SOURCE=SINK*(F2*SINK)
WRITE(6,20)

VALUES OF F1,F2,SINK AND SOURCE STRENGTHS ARE: //

F1,F2,SINK,SOURCE

A=.2
DO 30 I=1,5
U(I,1)=(-1.)*C-A*ALOG(ABS(A-C))+A*ALOG(ABS(A))+
C*(ALOG(ABS(A-C))-ALOG(ABS(A)))
A=A+.3
30 CONTINUE

A=.2
DO 40 I=1,5
U(I,2)=-.5*(A-C)**2+2.*A*(A-C)-A**2*ALOG(ABS(A-C))
+.5*A**2 - 2.*A**2 + A**2*ALOG(ABS(A)) +
2.*C*(C+A*ALOG(ABS(A-C))-A*ALOG(ABS(A)))-
C**2*(ALOG(ABS(A-C))-ALOG(ABS(A)))


```

57      A=A+.3
58      40 CONTINUE
59      C
60      A=.2
61      DO 50 I=1,5
62      U(1,3)=(-1./3.)*C**3-A**3*ALOG(ABS(A-C))-A*(.5*C**2
63      +A*C      )+A**3*ALOG(ABS(A))      -3.*C*
64      (-.5*(A-C)**2+2.*A*(A-C)-A**2*ALOG(ABS(A-C))+.5*A**2 -
65      C      2.*A**2 + A**2*ALOG(ABS(A))) - 3.*C**2*
66      C      (C+A*ALOG(ABS(A-C)) - A*ALOG(ABS(A))) +
67      C      C**3*(ALOG(ABS(A-C))-ALOG(ABS(A)))
68      A=A+.3
69      50 CONTINUE
70      C
71      A=.2
72      DO 51 I=1,5
73      U(1,4)=(-1.)*(C**4/4. + (A*C**3)/3.
74      C      + (A**2*C**2)/2. + A**3*C
75      C      + A**4*ALOG(ABS(A-C))-A**4*ALOG(ABS(A)))
76      C      +4.*C*(C**3/3.+(A*C**2)/2.+A**2*C
77      C      +A**3*ALOG(ABS(A-C))-A**3*ALOG(ABS(A)))
78      C      +6.*C**2*(-.5*(A-C)**2+2.*A*(A-C)
79      C      -A**2*ALOG(ABS(A-C))+.5*A**2-2.*A**2
80      C      +A**2*ALOG(ABS(A)))+4.*C**3*(C+
81      C      A*ALOG(ABS(A-C))-A*ALOG(ABS(A)))
82      C      -C**4*(ALOG(ABS(A-C))-ALOG(ABS(A)))
83      A=A+.3
84      51 CONTINUE
85      C
86      A=.2
87      DO 52 I=1,5
88      U(1,5)=(-1.)*(C**5/5.+(A*C**4)/4.+(A**2*C**3)/3.+
89      C      (A**3*C**2)/2.+A**4*C+
90      C      A**5*ALOG(ABS((A-C)/A)))+5.*C*
91      C      (C**4/4.+(A*C**3)/3.+(A**2*C**2)/2.+
92      C      A**3*C+A**4*ALOG(ABS((A-C)/A)))=
93      C      10.*C**2*(C**3/3.+(A*C**2)/2.+A**2*C+
94      C      A**3*ALOG(ABS((A-C)/A)))+10.*C**3*
95      C      (.5*(A-C)**2-2.*A*(A-C)+(3.*A**2)/2.+
96      C      A**2*ALOG(ABS((A-C)/A)))-5.*C**4*
97      C      (C+A*ALOG(ABS((A-C)/A)))+
98      C      C**5*ALOG(ABS((A-C)/A))
99      A=A+.3
100     52 CONTINUE
101     C
102     A=.2
103     STBOT=100.
104     NBOT=101
105     LRBOT=0.0
106     URBOT=8L
107     INCR0T=(URBOT-LRBOT)/STBOT
108     DO 40 I=6,10
109     SUM=0.0
110     NUMB=0
111     X12=LRBOT
112     DO 70 J=1,5
113     SUM=0.0

```

```

114 NUMBR=0
115 X12=LRBOT
116 DO 80 K=1,NBOT
117 IF (1.EQ.6) THEN
118 TOP=(X12-BL)*(COS(ATAN(H/(A-X3-X12))))
119 ELSE IF (1.EQ.7) THEN
120 TOP=(X12-BL)**2*(COS(ATAN(H/(A-X3-X12))))
121 ELSE IF (1.EQ.8) THEN
122 TOP=(X12-BL)**3*(COS(ATAN(H/(A-X3-X12))))
123 ELSE IF (1.EQ.9) THEN
124 TOP=(X12-BL)**4*(COS(ATAN(H/(A-X3-X12))))
125 ELSE IF (1.EQ.10) THEN
126 TOP=(X12-BL)**5*(COS(ATAN(H/(A-X3-X12))))
127 END IF
128 BOT=SQRT((A-X3-X12)**2 + H**2)
129 DIV=TOP/BOT
130 NUMBR=NUMBR+1
131 IF ((NUMBR.EQ.1).OR.(NUMBR.EQ.NBOT)) THEN
132 SUM=SUM+DIV
133 ELSE
134 TEMP=DIV*2.0
135 SUM=SUM+TEMP
136 END IF
137 X12=X12+INCBOT
138 80 CONTINUE
139 U(J,1)=SUM*(INCBOT/2.)
140 A=A+.3
141 70 CONTINUE
142 A=.2
143 60 CONTINUE
144 C
145 A=.2
146 STTOP=100.
147 NTOP=101
148 LBTOP=0.0
149 UBTOP=C
150 INCTOP=(UBTOP-LBTOP)/STTOP
151 C
152 DO 90 I=1,5
153 SUM=0.0
154 NUMBR=0
155 X11=LBTOP
156 DO 100 J=A,10
157 SUM=0.0
158 NUMBR=0
159 X11=LBTOP
160 DO 110 K=1,NTOP
161 IF (1.EQ.1) THEN
162 TOP=(X11-C)*(COS(ATAN(H/(A-X11))))
163 ELSE IF (1.EQ.2) THEN
164 TOP=(X11-C)**2*(COS(ATAN(H/(A-X11))))
165 ELSE IF (1.EQ.3) THEN
166 TOP=(X11-C)**3*(COS(ATAN(H/(A-X11))))
167 ELSE IF (1.EQ.4) THEN
168 TOP=(X11-C)**4*(COS(ATAN(H/(A-X11))))
169 ELSE IF (1.EQ.5) THEN
170 TOP=(X11-C)**5*(COS(ATAN(H/(A-X11))))

```

```

171      END IF
172      BOT=SQRT((A-X11)**2 + H**2)
173      DIV=TOP/BOT
174      NUMBR=NUMBR+1
175      IF((NUMBR.EQ.1).OR.(NUMBR.EQ.NTOP))THEN
176      SUM=SUM+DIV
177      ELSE
178      TEMP=DIV*2.0
179      SUM=SUM+TEMP
180      END IF
181      X11=X11 + INCTOP
182      CONTINUE
183      U(J,1)= SUM*(INCTOP/2.)
184      A=A+.3
185      100 CONTINUE
186      A=.2
187      90 CONTINUE
188      C
189      A=.2
190      DO 120 I=6,10
191      U(I,6)=(-1.)*BL - (A-X3)*ALOG(ABS(A-X3-BL)) +
192      C      (A-X3)*ALOG(ABS(A-X3)) - BL*((-1.)*
193      C      ALOG(ABS(A-X3-BL)) + ALOG(ABS(A-X3)))
194      A=A+.3
195      120 CONTINUE
196      C
197      A=.2
198      DO 130 I=6,10
199      U(I,7)=-0.5*(A-X3-BL)**2 + 2.*(A-X3)*(A-X3-BL)
200      C      - (A-X3)**2*ALOG(ABS(A-X3-BL)) + .5*(A-X3)**2
201      C      - 2.*(A-X3)**2 + (A-X3)**2*ALOG(ABS(A-X3)) +
202      C      2.*BL*(BL+(A-X3)*ALOG(ABS(A-X3-BL))
203      C      - (A-X3)*ALOG(ABS(A-X3))) - BL**2*
204      C      (ALOG(ABS(A-X3-BL)) - ALOG(ABS(A-X3)))
205      A=A+.3
206      130 CONTINUE
207      C
208      A=.2
209      DO 140 I=6,10
210      U(I,8)=(-1./3.)*BL**3 -(A-X3)**3*ALOG(ABS(A-X3-BL))
211      C      - (A-X3)*(1.5*BL**2 + (A-X3)*BL ) +
212      C      (A-X3)**3*ALOG(ABS(A-X3)) - 3.*BL*
213      C      (-.5*(A-X3-BL)**2 + 2.*(A-X3)*(A-X3-BL) -
214      C      (A-X3)**2*ALOG(ABS(A-X3-BL)) + .5*(A-X3)**2 -
215      C      2.*(A-X3)**2 + (A-X3)**2*ALOG(ABS(A-X3))) -
216      C      3.*BL**2*(BL+(A-X3)*ALOG(ABS(A-X3-BL))
217      C      - (A-X3)*ALOG(ABS(A-X3))) + BL**3*(ALOG(ABS(
218      C      A-X3-BL)) - ALOG(ABS(A-X3)))
219      A=A+.3
220      140 CONTINUE
221      C
222      A=.2
223      DO 141 I=6,10
224      U(I,9)=(-1.)*(BL**4/4. + ((A-X3)*BL**3)/3.
225      C      + ((A-X3)**2*BL**2)/2. + (A-X3)**3*BL+(A-X3)**4
226      C      *ALOG(ABS(A-X3-BL))-(A-X3)**4*ALOG(ABS(A-X3)))
227      C      +4.*BL*(BL**3/3.+(A-X3)*BL**2)/2.+(A-X3)**2

```

```

228      C      *BL*(A-X3)**3*ALOG(ABS(A-X3-BL))-(A-X3)**3
229      C      *ALOG(ABS(A-X3)))+6.*C**2*(-.5*(A-X3-BL)**2+2.*(A-X3)
230      C      *(A-X3-BL)-(A-X3)**2*ALOG(ABS(A-X3-BL))
231      C      +.5*(A-X3)**2-2.*(A-X3)**2
232      C      +(A-X3)**2*ALOG(ABS(A-X3)))+4.*BL**3*(BL+
233      C      (A-X3)*ALOG(ABS(A-X3-BL))-(A-X3)*ALOG(ABS(A-X3)))
234      C      -BL**4*(ALOG(ABS(A-X3-BL))-ALOG(ABS(A-X3)))
235      A=A+.3
236      141 CONTINUE
237      C
238      A=.2
239      DO 142 J=6,10
240      U(1,10)=(-1.)*(RL**5/5.+(A-X3)*BL**4)/4.+(A-X3)**2*BL**3)/3.+
241      C      ((A-X3)**3*BL**2)/2.+(A-X3)**4*BL+
242      C      (A-X3)**5*ALOG(ABS((A-X3)-BL)/(A-X3)))+5.*BL*
243      C      (BL**4/4.+(A-X3)*BL**3)/3.+(A-X3)**2*BL**2)/2.+
244      C      (A-X3)**3*BL+(A-X3)**4*ALOG(ABS((A-X3)-BL)/(A-X3)))-
245      C      10.*RL**2*(BL**3/3.+(A-X3)*RL**2)/2.+(A-X3)**2*BL+
246      C      (A-X3)**3*ALOG(ABS((A-X3)-BL)/(A-X3)))+10.*BL**3*
247      C      (.5*(A-X3)-BL)**2-2.*(A-X3)*((A-X3)-BL)+(3.*(A-X3)**2)/7
248      C      (A-X3)**2*ALOG(ABS((A-X3)-BL)/(A-X3)))-5.*BL**4*
249      C      (BL+(A-X3)*ALOG(ABS((A-X3)-BL)/(A-X3)))+
250      C      BL**5*ALOG(ABS((A-X3)-BL)/(A-X3)))
251      A=A+.3
252      142 CONTINUE
253      C
254      WRITE(6,150)
255      150 FORMAT(' THE U MATRIX IS: '/')
256      DO 160 I=1,10
257      WRITE(6,*) (U(I,J),J=1,10)
258      160 CONTINUE
259      C
260      C      ASSIGN THE CONSTANTS ASSOC WITH SINK AND SOURCE
261      C
262      A=.2
263      DO 170 I=1,5
264      N(I)=(-1.)*(SOURCE*(Y1/(A**2-2.*X2*A+X2**2+Y1**2))-
265      C      SINK*(Y1/(A**2-2.*X1*A+X1**2+Y1**2)))
266      A=A+.3
267      170 CONTINUE
268      A=.2
269      DO 180 J=6,10
270      N(J)=(-1.)*(SOURCE*(Y2/(A**2-2.*X2*A+X2**2+Y2**2))-
271      C      SINK*(Y2/(A**2-2.*X1*A+X1**2+Y2**2)))
272      A=A+.3
273      180 CONTINUE
274      WRITE(6,190)
275      190 FORMAT(' THE N ARRAY IS: '/')
276      DO 200 I=1,10
277      WRITE(6, '(1X,12,3X,F20.8)') I,N(I)
278      200 CONTINUE
279      C
280      C
281      CALL INVDFT(U,10,DTNRH,DETH)
282      WRITE(6,210)
283      210 FORMAT(' THE INVERTED U MATRIX IS: ')
284      DO 220 I=1,10

```

```

285      WRITE(6,*) (U(I,J), J=1,10)
286      220 CONTINUE
287      C
288      C
289      DO 230 I=1,10
290      AB(I)=U(I,1)*N(1)+U(I,2)*N(2)+U(I,3)*N(3)+
291      C      U(I,4)*N(4)+U(I,5)*N(5)+U(I,6)*N(6)
292      C      +U(I,7)*N(7)+U(I,8)*N(8)
293      C      +U(I,9)*N(9)+U(I,10)*N(10)
294      230 CONTINUE
295      WRITE(6,240)
296      240 FORMAT(' THE COEFFS, A1, A2, A3, A4, A5, B1, B2, B3, B4, B5 ARE: '/')
297      DO 250 I=1,10
298      WRITE(6, '(1X, F20.8)') AB(I)
299      250 CONTINUE
300      C
301      C      NOW FOR THE LIFT CALCULATION
302      C
303      NLIFT=100.0
304      STEPL=100
305      SUM=0.0
306      TEMP=0.0
307      NUMBR=0
308      X=0.0
309      INCL1=(C-0.0)/NLIFT
310      DO 260 I=1, STEPL+1
311      GAMMA1=AB(1)*(X-C)+AB(2)*((X-C)**2)+AB(3)*((X-C)**3)
312      C      +AB(4)*((X-C)**4)+AB(5)*((X-C)**5)
313      C
314      C
315      WRITE(3,270) X, GAMMA1
316      270 FORMAT(1X, 2F16.8)
317      C
318      C
319      NUMBR=NUMBR+1
320      IF ((NUMBR.EQ. 1) .OR. (NUMBR.EQ. STEPL+1)) THEN
321      SUM=SUM+GAMMA1
322      ELSE
323      TEMP=GAMMA1*2.0
324      SUM=SUM+TEMP
325      END IF
326      X=X+INCL1
327      260 CONTINUE
328      L1=SUM*(INCL1/2.)
329      WRITE(6,280)
330      280 FORMAT(' THE VORTICITY OF THE TOP PLATE IS: '/')
331      WRITE(6, '(1X, F20.10)') L1
332      SUM=0.0
333      TEMP=0.0
334      NUMBR=0
335      C
336      C
337      X=0.0
338      INCL2=(X4-X3)/NLIFT
339      DO 290 I=1, STEPL+1
340      GAMMA2=AB(6)*(X-BL)+AB(7)*(X-BL)**2+AB(8)*(X-BL)**3
341      C      +AB(9)*(X-BL)**4+AB(10)*(X-BL)**5

```

```

342 C
343 C
344 WRITE(11,300) X,GAMMA2
345 300 FORMAT(1X,2F16.8)
346 C
347 C
348 NUMBR=NUMBR+1
349 IF ((NUMBR.EQ. 1) .OR. (NUMBR.EQ. STEPL+1)) THEN
350 SUM=SUM+GAMMA2
351 ELSE
352 TEMP=GAMMA2*2.0
353 SUM=SUM+TEMP
354 END IF
355 X=X+INCL2
356 290 CONTINUE
357 L2=SUM*(INCL2/2.)
358 WRITE(6,310)
359 310 FORMAT(' THE VORTICITY OF THE BOTTOM PLATE IS: '/')
360 WRITE(6, '(1X,F20.10)') L2
361 LIFT=(RHO*VEL)*(L1+L2)
362 WRITE(6,320)
363 320 FORMAT(' THE VALUE OF THE LIFT IS: '/')
364 WRITE(6, '(1X,F14.8)') LIFT
365 C
366 C THIS IS THE CHECK PORTION OF THE PROGRAM
367 C
368 C1=(-1.)*AR(5)
369 C2=AB(4)-5.*C*AB(5)
370 C3=AR(3)-4.*C*AB(4)+10.*C**2*AB(5)
371 C4=AR(2)-3.*C*AR(3)+6.*C**2*AB(4)-10.*C**3*AB(5)
372 C5=AR(1)-2.*C*AR(2)+3.*C**2*AR(3)-
373 C 4.*C**3*AB(4)+5.*C**4*AB(5)
374 C6=C*AR(1)-C**2*AB(2)+C**3*AB(3)-C**4*AB(4)+
375 C C**5*AR(5)
376 C7=(-1.)*AB(10)
377 C8=AB(9)-5.*BL*AR(10)
378 C9=AB(8)-4.*BL*AB(9)+10.*BL**2*AB(10)
379 C10=AB(7)-3.*BL*AB(8)+6.*BL**2*AB(9)-10.*BL**3*AB(10)
380 C11=AB(6)-2.*BL*AB(7)+3.*BL**2*AB(8)-
381 C 4.*BL**3*AB(9)+5.*BL**4*AB(10)
382 C12=BL*AB(6)-BL**2*AB(7)+BL**3*AB(8)-BL**4*AB(9)+
383 C BL**5*AB(10)
384 C
385 C FOR THE TOP PLATE WE HAVE:
386 C
387 WRITE(6,500)
388 500 FORMAT(' V,U AND PRESSURE ALONG THE TOP PLATE: '/')
389 X=0.05
390 DO 321 I=1,20
391 P1(I)=SOURCE*(Y1/(X**2-2.*X2*X+X2**2+Y1**2))
392 C
393 P9(I)=(SOURCE/(2.*P1))*(X-X2)/(X**2-2.*X2*X+X2**2+Y1**2))
394 C
395 P2(I)=(-1.)*(SINK*(Y1/(X**2-2.*X1*X+X1**2+Y1**2)))
396 C
397 P10(I)=((-1.*SINK)/(2.*P1))*(X-X1)/(X**2-2.*X1*X+X1**2+Y1**2))
398 C

```

```

399      P3(I)=C1*(C**5/5.+(X*C**4)/4.+(X**2*C**3)/3.+(X**3*C**2)/2.+
400      C      X**4*C+X**5*ALOG(ABS((X-C)/X)))-
401      C      C2*(C**4/4.+(X*C**3)/3.+(X**2*C**2)/2.+
402      C      X**3*C+X**4*ALOG(ABS((X-C)/X)))-
403      C      C3*(C**3/3.+(X*C**2)/2.+X**2*C+
404      C      X**3*ALOG(ABS((X-C)/X)))-C4*(C**2/2.+
405      C      X*C+X**2*ALOG(ABS((X-C)/X)))-C5*(X*
406      C      ALOG(ABS((X-C)/X))+C)+C6*ALOG(ABS((X-C)/X))
407      C
408      SUM=0.0
409      TEMP=0.0
410      X12=0.0
411      C
412      DO 322 K=1,101
413      TOP=(AB(6)*(X12-BL)+AB(7)*(X12-BL)**2+
414      C      AB(8)*(X12-BL)**3+AB(9)*(X12-BL)**4+
415      C      AB(10)*(X12-BL)**5)*(COS(ATAN(H/(X-X3-X12))))
416      BOT=SQRT((X-(X12+X3))**2+H**2)
417      DIV=TOP/BOT
418      C
419      IF((K.EQ. 1) .OR. (K.EQ. 101)) THEN
420      SUM=SUM+DIV
421      ELSE
422      TEMP=DIV*2.
423      SUM=SUM+TEMP
424      END IF
425      C
426      X12=X12+.01
427      322 CONTINUE
428      C
429      P4(I)=SUM*(.01/2.)
430      C
431      SUM=0.0
432      TEMP=0.0
433      X12=0.0
434      C
435      DO 324 K=1,101
436      TOP=(AB(6)*(X12-BL)+AB(7)*(X12-BL)**2+
437      C      AB(8)*(X12-BL)**3+AB(9)*(X12-BL)**4+
438      C      AB(10)*(X12-BL)**5)*(SIN(ATAN(H/(X-X3-X12))))
439      BOT=SQRT((X-(X12+X3))**2+H**2)
440      DIV=TOP/BOT
441      C
442      IF((K.EQ. 1) .OR. (K.EQ. 101)) THEN
443      SUM=SUM+DIV
444      ELSE
445      TEMP=DIV*2.
446      SUM=SUM+TEMP
447      END IF
448      C
449      X12=X12+.01
450      324 CONTINUE
451      C
452      P11(I)=(1./(2.*PI))*SUM*(.01/2.)
453      C
454      VTOP(I)=P1(I)+P2(I)+P3(I)+P4(I)
455      UTOP(I)=VEL+P9(I)+P10(I)+P11(I)

```

```

456 C      PTOP(I)=(.5*RHO*VEL**2)*(1.-((UTOP(I)**2+VTOP(I)**2)/
457      (VEL**2)))*PRES
458 C
459      WRITE(6,373) X,VTOP(I),UTOP(I),PTOP(I)
460      X=X+.05
461 321 CONTINUE
462 C
463 C      FOR THE BOTTOM PLATE WE HAVE:
464 C
465      WRITE(6,600)
466 600 FORMAT(' V,U AND PRESSURE ALONG THE BOTTOM PLATE')
467      X=0.6
468      DO 330 I=1,20
469      P5(I)=SNURCF*(Y2/(X**2-2.*X2*X+X2**2+Y2**2))
470 C
471      P12(I)=(SOURCE/(2.*PI))*((X-X2)/(X**2-2.*X2*X+X2**2+Y2**2))
472 C
473      P6(I)=(-1.)*(SINK*(Y2/(X**2-2.*X1*X+X1**2+Y2**2)))
474 C
475      P13(I)=((-1.*SINK)/(2.*PI))*((X-X1)/(X**2-2.*X1*X+X1**2+Y2**2))
476 C
477      P8(I)=C7*(BL**5/5.+((X-X3)*BL**4)/4.+((X-X3)**2*BL**3)/3.
478      +((X-X3)**3*BL**2)/2.+
479      (X-X3)**4*BL+(X-X3)**5*ALOG(ABS((X-X3-BL)/(X-X3))))-
480      C8*(BL**4/4.+((X-X3)*BL**3)/3.+((X-X3)**2*BL**2)/2.+
481      (X-X3)**3*BL+(X-X3)**4*ALOG(ABS((X-X3-BL)/(X-X3))))-
482      C9*(BL**3/3.+((X-X3)*BL**2)/2.+(X-X3)**2*BL+
483      (X-X3)**3*ALOG(ABS((X-X3-BL)/(X-X3))))-C10*(BL**2/2.+
484      (X-X3)*BL+(X-X3)**2*ALOG(ABS((X-X3-BL)/(X-X3))))
485      -C11*((X-X3)*ALOG(ABS((X-X3-BL)/(X-X3)))
486      +BL)+C12*ALOG(ABS((X-X3-BL)/(X-X3)))
487 C
488      SUM=0.0
489      TEMP=0.0
490      X11=0.0
491 C
492      DO 331 K=1,101
493      TOP=(AB(1)*(X11-C)+AB(2)*(X11-C)**2+
494      AB(3)*(X11-C)**3+AB(4)*(X11-C)**4+
495      AB(5)*(X11-C)**5)*(COS(ATAN(H/(X-X11))))
496      BOT=SQRT((X-X11)**2+H**2)
497      DIV=TOP/BOT
498 C
499      IF((K.EQ. 1).OR.(K.EQ. 101)) THEN
500      SUM=SUM+DIV
501      ELSE
502      TEMP=DIV*2.
503      SUM=SUM+TEMP
504      END IF
505 C
506      X11=X11+.01
507 331 CONTINUE
508 C
509      P7(I)=SUM*(.01/2.)
510 C
511      SUM=0.0
512      TEMP=0.0

```



```

513      X11=0.0
514      C
515          DO 332 K=1,101
516      TOP=(AB(1)*(X11-C)+AB(2)*(X11-C)**2+
517      C      AB(3)*(X11-C)**3+AB(4)*(X11-C)**4+
518      C      AB(5)*(X11-C)**5*(SIN(ATAN(H/(X-X11))))
519      BOT=SQRT((X-X11)**2+H**2)
520      DIV=TOP/BOT
521      C
522      IF((K.EQ. 1) .OR. (K.EQ. 101)) THEN
523      SUM=SUM+DIV
524      ELSE
525      TEMP=DIV*2.
526      SUM=SUM+TEMP
527      END IF
528      C
529      X11=X11+.01
530      332 CONTINUE
531      C
532      P14(1)=(1./(2.*PI))*SUM*(.01/2.)
533      C
534      VBOT(1)=P5(1)+P6(1)+P7(1)+P8(1)
535      UBOT(1)=VEL+P12(1)+P13(1)+P14(1)
536      PBOT(1)=(.5*RHO*VEL**2)*(1.-((UBOT(1)**2+VBOT(1)**2)/
537      C      (VEL**2)))+PRES
538      WRITE(6,323) X,VBOT(1),UBOT(1),PBOT(1)
539      X=X+.05
540      330 CONTINUE
541      C
542      323 FORMAT(1X,4F16.5)
543      END
544      SUBROUTINE INVDET(C,N,DTHRM,DETM)
545      DIMENSION C(N,N), J(100)
546      PD=1.
547      DO 124 L=1,N
548      DD=0.
549      DO 123 K=1,N
550      123 DD=DD+C(L,K)*C(L,K)
551      DD=SQRT(DD)
552      124 PD=PD*DD
553      DETM=1.
554      DO 125 L=1,N
555      125 J(L+20)=L
556      DO 144 L=1,N
557      CC=0.
558      M=L
559      DO 135 K=L,N
560      IF ((ABS(CC)-ABS(C(L,K))) .GE. 0.) GO TO 135
561      126 M=K
562      CC=C(L,K)
563      135 CONTINUE
564      127 IF (L.EQ.M) GO TO 138
565      128 K=J(M+20)
566      J(M+20)=J(L+20)
567      J(L+20)=K
568      DO 137 K=1,N
569      S=C(K,L)

```

```

570      C(K,L)=C(K,M)
571      137 C(K,M)=S
572      138 C(L,L)=1.
573      DETM=DETM*CC
574      DO 139 M=1,N
575      139 C(L,M)=C(L,M)/CC
576      DO 142 M=1,N
577      IF (L.EQ.M) GO TO 142
578      129 CC=C(M,L)
579      IF (CC.EQ.0.) GO TO 142
580      130 C(M,L)=0.
581      DO 141 K=1,N
582      141 C(M,K)=C(M,K)-CC*C(L,K)
583      142 CONTINUE
584      144 CONTINUE
585      DO 143 L=1,N
586      IF (J(L+20).EQ.L) GO TO 143
587      131 M=L
588      132 M=M+1
589      IF (J(M+20).EQ.L) GO TO 133
590      136 IF (N.GT.M) GO TO 132
591      133 J(M+20)=J(L+20)
592      DO 163 K=1,N
593      CC=C(L,K)
594      C(L,K)=C(M,K)
595      163 C(M,K)=CC
596      J(L+20)=L
597      143 CONTINUE
598      DETM=ABS(DETM)
599      DTNRH=DETM/PD
600      RETURN
601      END

```

VITA

John T. Domalski was born in Toledo, Ohio on 16 May 1950. He attended Saint Francis de Sales High School there and graduated in 1968. He later attended Purdue University, West Lafayette, Indiana, and graduated in 1972 with a Bachelor of Science degree from the School of Interdisciplinary Engineering. The curriculum pursued at Purdue involved a combination of basic engineering and journalism studies to form a technical writing major. He was employed following graduation by the Central Intelligence Agency as an imagery analyst and later, in September 1978, was assigned to Wright-Patterson Air Force Base, Ohio as liaison officer to the Foreign Technology Division. He began studies at AFIT as a part-time student in April 1979 in the Aero/Astro Department; pursuing the sequences of Air Breathing Propulsion and Air Weapons Delivery. He presently works for the Foreign Technology Division as an analyst of tactical weapon systems. He married the former Janice Goebel of East Jordan, Michigan in 1972, and they have two daughters; Emily (age 4) and Elizabeth (age 1).

Permanent Address: 4589 Falcon Circle
Dayton, Ohio 45424

UNCLASSIFIED

SECURITY CLASSIFICATION OF THIS PAGE (When Data Entered)

REPORT DOCUMENTATION PAGE		READ INSTRUCTIONS BEFORE COMPLETING FORM
1. REPORT NUMBER AFIT/GAE-82D-10	2. GOVT ACCESSION NO. AD-A124695	3. RECIPIENT'S CATALOG NUMBER
4. TITLE (and Subtitle) THEORETICAL DETERMINATION OF THE LIFT OF A SIMULATED EJECTOR WING		5. TYPE OF REPORT & PERIOD COVERED MS THESIS, JAN-DEC 82
		6. PERFORMING ORG. REPORT NUMBER
7. AUTHOR(s) JOHN T. DOMALSKI		8. CONTRACT OR GRANT NUMBER(s)
9. PERFORMING ORGANIZATION NAME AND ADDRESS AIR FORCE INSTITUTE OF TECHNOLOGY (AFIT-EN) WRIGHT-PATTERSON AFB, OHIO 45433		10. PROGRAM ELEMENT, PROJECT, TASK AREA & WORK UNIT NUMBERS
11. CONTROLLING OFFICE NAME AND ADDRESS		12. REPORT DATE DECEMBER 1982
		13. NUMBER OF PAGES 73
14. MONITORING AGENCY NAME & ADDRESS (if different from Controlling Office)		15. SECURITY CLASS. (of this report) UNCLASSIFIED
		15a. DECLASSIFICATION/DOWNGRADING SCHEDULE
16. DISTRIBUTION STATEMENT (of this Report) APPROVED FOR PUBLIC RELEASE; DISTRIBUTION UNLIMITED		
17. DISTRIBUTION STATEMENT (of the abstract entered in Block 20, if different from Report)		
18. SUPPLEMENTARY NOTES Approved for public release: IAW AFR 100-17, LYNN E. WOLAVER Dean for Research and Professional Development Air Force Institute of Technology (ATC) Wright-Patterson AFB OH 45433 19 JAN 1983		
19. KEY WORDS (Continue on reverse side if necessary and identify by block number) EJECTOR WING AIRFOIL THEORY		
20. ABSTRACT (Continue on reverse side if necessary and identify by block number) THE SOLUTION PROCEDURE AND SUPPORTING THEORY HAVE BEEN DEVELOPED FOR CALCULATION OF THE LIFT PER UNIT SPAN OF AN EJECTOR WING MODEL. MODEL CONSISTS OF TWO VORTEX SHEETS, A POINT SINK AND A POINT SOURCE IN A UNIFORM STREAM. SOLUTION IS SHOWN TO BE DEPENDENT ON THE NUMBER OF CONTROL POINTS USED AND EXAMPLES USING FIVE CONTROL POINTS ARE PRESENTED. A FORTRAN COMPUTER PROGRAM FOR THE FIVE-CONTROL-POINT CASE IS PRESENTED.		

DD FORM 1 JAN 73 1473 EDITION OF 1 NOV 65 IS OBSOLETE

UNCLASSIFIED

SECURITY CLASSIFICATION OF THIS PAGE (When Data Entered)